MELISSA TEMKOV

OPTOFLUIDIC DETECTION OF AQUEOUS AMMONIA AND PARASITIC CYSTS

By MELISSA TEMKOV, B.Sc.

A Thesis Submitted to the School of Graduate Studies in Partial Fulfilment of the Requirements for the Degree Master of Applied Science

McMaster University MASTER OF APPLIED SCIENCE (2022) Hamilton, Ontario (History)

TITLE: Optofluidic Detection of Aqueous Ammonia and Parasitic (Oo)cysts AUTHOR: Melissa Temkov, B. Sc. (Towson University) SUPERVISOR: Professor Q. Fang NUMBER OF PAGES: xii, 104

Water quality monitoring for remote and Indigenous communities is needed to provide safe water to all. Detection of aqueous ammonia by fluorescent hydrogel, and parasitic cysts by flow analysis, provides a low-cost, point-of-care detection mechanism. A fluorescence responsive hydrogel for aqueous ammonia detection was produced and the essential components for ammonia responsiveness were determined. Detection mechanisms of parasites *Cryptosporidium* and *Giardia*, two of the most prevalent parasitic protozoans causing human gastrointestinal illness, were analyzed and compared. Baseline images of the parasitic (oo)cysts were captured by conventional microscopy for the training of particle tracking algorithms to be implemented into a microfluidic device. The microfluidic device detection mechanism will utilize shadow imaging and flow analysis to detect parasitic (oo)cysts.

Water quality monitoring in Canada is essential to providing safe water to all. Indigenous and remote communities, many of which are under boiling drinking water advisories, lack availability and/or funding to water monitoring resources. A low-cost, point-of-care detection mechanism has been proposed for the detection of aqueous ammonia and protozoan parasites, which affect the safety of a source of water. An ammonia fluorescence responsive hydrogel, based on the fluorescence quenching of rare earth metal Europium (Eu^{3+}) upon contact with aqueous ammonia, has been proposed to be incorporated into a microfluidic device, which utilizes shadow imaging and flow analysis to detect parasitic (oo)cysts of *Cryptosporidium* and *Giardia*, two of the most prevalent protozoan parasites which cause gastrointestinal illness around the world. Fabrication of the ammonia sensitive hydrogel was completed, and the essential components to the ammonia sensitivity were determined. Chemical analysis and solvent modifications found that Formamide is the essential solvent to maintain ammonia sensitivity. A literature review into the current detection mechanisms of *Cryptosporidium* and *Giardia* was completed to provide a reference and starting point for the development of the low-cost, point-of-care device proposed in this thesis. Baseline images of *Cryptosporidium parvum* and *Giardia lamblia* were captured to provide a reference for the development of a particle tracking algorithm to be used in the microfluidic device. The images captured highlight morphological features essential to developing a tracking mechanism based on the morphology of the (oo)cysts.

I would like to thank my committee, Dr. Kim and Dr. Schellhorn for advising me in directions to follow and providing me with constant feedback towards how to be a better researcher.

I would like to thank all the friends I made along the journey through my Masters. Ian, Tianqi, Zach, Trevor, Antonin, and Clement, your assistance and support have helped me to strive to be a better researcher and human being. Your friendship and love have kept me sane.

I would like to thank my family, my mom, my grandparents, my brother, and David for pushing me to pursue my second degree, and for being my biggest supporters throughout the many difficulties I have faced.

Finally, I would like to thank Dr. Fang for being there for me both within the academic world and without, you have supported me through this entire process. Thank you for teaching me skills that will help me in my future scientific endeavors, and for consistently caring about me not only as a researcher, but as a person. The lessons you have taught me are invaluable.

TABLE OF CONTENTS

LIST OF ABBREVIATIONS AND SYMBOLS

AN Bourns Science Building	ABB
Auramine-phenol	AP
Biological safety cabinet	BSC
Bis(trimethylsilyl)acetamide	BSA
Clustered regularly interspaced short palindromic repeats	CRISPR
Complimentary DNA	cDNA
Complimentary RNA	cRNA
Degrees Celsius	^{O}C
Deionized	DI
Deoxyribonucleic acid	DNA
Differential intereference contrast	DIC
Dimethyl sulfoxide	DMSO
Direct immunofluorescence assay	DIFA
Droplet digital PCR	ddPCR
Electrochemical impedance spectroscopy	EIS
Electrophoretic mutation scanning	EMS
Enzyme-linked immunoabsorbent assay	ELISA
Enzyme-linked immuno-culture assay	ELICA
Fluorescein-5-isothiocyanate	FITC
Fluorescence activated cell sorting	FACS
Fluorescence in-situ hybridization	FISH
Formamide	Fm
Irritable bowel syndrome	IBS
Indirect immunofluorescence assay	IIFA
Laser-scanning cytometry	LSC
Light emitting diode	LED
Limit of detection	LOD
Loop-mediated isothermal amplification	LAMP
Messenger RNA	mRNA
Monoclonal antibody	MAB
Nucleic acid sequence-based amplification	NASBA
Polycarbonate track etched membrane filter to concentrate	PTCE
o-phthalaldehyde	OPA
Phase contrast	PC
Point-of-Care	POC
Poly(vinyl alcohol)	PVA
Polydimethylsiloxane	PDMS
Polylactic acid	PLA
Polymerase chain reaction	PCR
Power of hydrogen	pH

Quantum dot	QD
Real-time PCR	qPCR
Reactive arthritis	RA
Restriction fragment length polymorphism assay PCR	RFLP-PCR
Reverse-transcriptase PCR	RT-PCR
Ribonucleic acid	RNA
Safranin-methylene blue	SMB
Salicylic acid	Sal
Scanning electron microscopy	SEM
self-assembled monolayers	SAMs
Sigma Aldrich	SA
Sodium Hydroxide	NaOH
Surface enhanced Raman spectroscopy	SERS
Surface plasmon resonance	SPR
Tandem affinity purification	TAP
Thenoyltrifluoroacetone	TTA
ThermoFisher Scientific	TF
Total internal reflection	TIRF
Traditional knowledge	TK
Ultra-violet	UV
Wright-Giesma	GDQ
Ziehl-Neelsen	ZN

LIST OF FIGURES AND TABLES

Chapter 1: Introduction

Since the beginning of the 21st century, there has been an increase in the amount of attention towards monitoring the Earth; climate change, natural disasters, population growth, and species extinction are some of the factors that have driven the discourse regarding the planet's sustainability into mainstream media.

Of the topics that have been brought to the forefront, water quality, especially in a natural resource rich country such as Canada, has been a top discussion area. Water is an essential resource for all life, which is often in short supply due to temporal and special constraints, and while Canada has the third largest supply of renewable freshwater in the world, the spread over which the abundant sources are allocated is uneven[1,2]. Environmental governance, which includes the governance of water, is highly decentralized in Canada[3]. Over a quarter of the nation's population relies on groundwater for drinking, which serves a problem as groundwater resources are not fully mapped, and as populations increase along the southern border, demand rises and heavily concentrates in specific areas [1,3] Natural Resources Canada is currently developing a water quality database baseline, which pulls data from at least 14 federal and provincial governments, conservation authorities, water boards, and private companies across the country[2]. In conjunction with the quality database, technologies are being developed to map groundwater in difficult to access areas, such as drones with density and temperature sensors, which will be used to create a more comprehensive outline of where drinking water sources are located. A map of freshwater resources is only one step towards minimizing water insecurity in Canada; water needs to be identified as safe or unsafe to consume and use for everyday purposes. As the databases continue to expand, there has been a call to develop low-cost systems capable of monitoring various analytes in water, particularly in remote locations and on Indigenous territories.

It has been repeatedly demonstrated that high quality water is a crucial piece of an effective socio-economic development plan[4]. Canada's fractionalized water management strategies have forced many Canadians into drinking water advisories, requiring individuals to boil household water or to purchase prepackaged water. With the rise of scrutiny regarding Canada's historical and current treatment of Indigenous populations, water quality and security have become a highlighted issue in the country's efforts to make amends and improve living conditions of Indigenous people, which contributes to the country's larger economic development plan.

Approximately one third of First Nations individuals living on reserves in Canada are faced each day with an increased threat of health conditions and waterborne infections caused by high-risk water systems, which affect at least 39 First Nations communities[5]. The likelihood of illness is much higher to Indigenous people than the Canadian national average[6]. 70 historic treaties, as well as 25 modern treaties, are currently in place between

the Crown and Indigenous peoples, with negotiations ongoing regarding the claim to land (Miller). These land claim negotiations are in part a product of the unevenly distributed water management strategies, with lack of infrastructure and access to fresh water giving rise to the need of new sources, which begs the requirement of water quality monitoring.

Natural lakes, rivers, and watersheds contain a multitude of organisms, chemicals, plants, and organism by-products which are of interest to explore and quantify for quality monitoring. Anthropogenic sources of chemical compounds contribute to fluctuating aquatic ecosystems and can result in harmful growth or destruction of delicate balances between organisms. There is currently still no widely accepted practical strategy to monitor water quality, despite the issue having been addressed in literature since the 1940s[7]. There are several biomarkers and biogeochemical markers that are related to the quality of water, such as salinity, nitrate concentration, pH, sedimentation, organic matter, heavy metals, and pesticide contamination. There is also no data reporting framework that is accepted Canada-wide to standardize reporting of such quality markers [2].

My masters research was designed to bridge the disconnect in water quality monitoring; my literature review chapter revolves around the detection mechanisms of parasitic cysts and waterborne illness needs of Indigenous communities, while my experimental work chapters are a step in the framework of bringing low-cost, point-of care devices to natural watersheds, from an optics-based method. The ultimate goal of the work I am taking part in is to design a system that allows for the monitoring of aqueous ammonia and parasitic cysts, without the need for trained technician collection of water samples. The ease of connection between the individual focuses on ammonia and parasitic cysts comes from the ability of both contaminants to be monitored optically.

Chapter 2 provided an overview and described various detection mechanisms by which C*ryptosporidium* and G*iardia* and their (oo)cysts can be detected in liquid and solid samples. This chapter provides a comparison to the proposed detection method outlined in the Parasitic Detection chapter. This chapter also touches on the state of Indigenous communities regarding water quality and healthcare related to waterborne conditions.

Chapter 3 outlines the ground truth imaging of *Cryptosporidium* and *Giardia*, done to establish a baseline for flow analysis in the completed proposed device. Microscopy studies were investigated prior to imaging to ensure the images would be relevant to aid in the production of particle tracking algorithms.

Chapter 4 details the work done towards a point-of-care, low-cost device for the monitoring of aqueous ammonia. Taken from a prior investigation on using a pH sensitive dye, an ammonia sensitive hydrogel was explored, and a prototype device was designed.

The final chapter (Chapter 5) concludes this chapter, summarizing and presenting the thesis in a way which ties together all prior chapters.

My work presented in this thesis establishes a comparison of detection mechanisms for which the proposed method in this thesis will be compared to, as well as the relevance of water quality monitoring and point-of-care healthcare for Indigenous communities, presented in Chapter 2. In Chapter 3, my work presents ground truth images for a particle tracking algorithm to be built off of, based on the morphology of (oo)cysts found while imaging on a microscope. Chapter 4 is the work towards developing a low-cost detection mechanism for aqueous ammonia, which could be combined with the *Cryptosporidium* and *Giardia* detection device.

1. McKitrick Ross, Aliakbari Elmira, Stedman Ashley. *Evaluating the State of Fresh Water in Canada*. (Aliakbari Elmira, McKitrick Ross, Stedman Ashley, eds.). Fraser Institute; 2018.

2. Miller CB, Cleaver A, Huntsman P, et al. Predicting water quality in Canada: mind the (data) gap. *Canadian Water Resources Journal*. 2021;47(4):169-175. doi:10.1080/07011784.2021.2004931

3. Bakker K, Cook C. Water Governance in Canada: Innovation and Fragmentation. *Water Resources Development*. 2011;27:275-289. doi:10.1080/07900627.2011.564969

4. Bartram J, Ballance R. Water Quality Monitoring - A Practical Guide to the Design and Implementation of Freshwater. *Quality Studies and Monitoring Programmes*. Published online 1996:1-348.

5. Wilson NJ, Montoya T, Arseneault R, Curley A. Governing water insecurity: navigating indigenous water rights and regulatory politics in settler colonial states. Published online 2021. doi:10.1080/02508060.2021.1928972

6. Soler P, Faria M, Barata C, García-Galea E, Lorente B, Vinyoles D. Improving water quality does not guarantee fish health: Effects of ammonia pollution on the behaviour of wild-caught pre-exposed fish. *PLoS One*. 2021;16(8):e0243404. doi:10.1371/journal.pone.0243404

7. Behmel S, Damour M, Ludwig R, Rodriguez MJ. Water quality monitoring strategies — A review and future perspectives. *Science of the Total Environment*. 2016;571:1312-1329. doi:10.1016/j.scitotenv.2016.06.235

Chapter 2: Cryptosporidium and Giardia

Cryptosporidium and *Giardia* are members of the apicomplexan protozoan parasite family; the parasites infect and cause gastrointestinal and respiratory illness in numerus vertebrae species, including humans[8–17]. The first human case of gastrointestinal disease that was determined to have been the result of *Cryptosporidium* infection occurred in the 1970s, despite the genus' first description by Tyzzer in 1910[9–12]. Antoine van Leeuwenhoek first described *Giardia* in 1681, after discovering motile organisms in his own stool[14,15]. Notwithstanding, the interest in studying both parasites did not increase until about the late 1970s to early 1980s. Both parasites lead to a significant rate of mortality and morbidity throughout the world, in both developed and developing countries.

As the demand for country-wide, clean, drinkable water is increasing, these parasites have become an interest to study for water quality. Understanding these parasites and what makes dangerous to humans and other mammals is key to finding a method of identifying the pathogenic species in water. In this approach, we must know which form of the parasites we are looking for and their morphology in order to identify them in a tested water sample.

2.1 Giardia and Giardiasis

Giardia intestinalis, also known as the species *G. duodenalis* or *G. lamblia*, is the most prevalent protozoan pathogen in the human intestinal tract that causes illness, which is estimated to cause around 280 million infections (giardiasis) annually[8,9,15–20]. Cases of *Giardiasis* usually onset acutely and typically resolve without the need for intervention, but in some cases can lead to chronic disease. Cases of human infection occur worldwide, with higher frequencies in locations where sanitation is poor.

The human pathogenic species of *Giardia* has two distinct assemblages (A and B), which cause considerable variation of infections between countries[17,18]. These strains are of interest to study not only for medical research, but also for water quality research, since *Giardia* is a major contributor to human protist induced illness. While *G. duodenalis* can infect a multitude of mammals, there are several species of *Giardia* which infect other mammals while they do not infect humans. Examples of these species are *Giardia canis* and *Giardia bovis*, which infect dogs and cows/sheep/alpacas/goats/pigs, respectively[15,16,18,19]. These species are also of interest to study, but as a secondary interest for water quality monitoring.

The symptoms of *Giardiasis* can range from asymptomatic to chronic diarrhea to malabsorption, which, in general, impact immunocompromised individuals and children

the most severely. Other symptoms can include bloating, and weight loss. Persons of all ages can be affected, but the most frequently affected age group is infants [9,14]. More recent implications of *Giardia* as a human disease have focussed on the impact of childhood growth, with a study showing that within the first 6 months of life, *Giardia* presence resulted in a decreased length-for-age Z score at the age of 2, by 0.4[9]. *Giardia* infections have the ability to alter the gut's microbiota; irritable bowel syndrome (IBS), lactose intolerance, and food allergies can be developed following a resolved case of *Giardia* infection[14,16,21]. It has also been shown that reactive arthritis (RA) can arise during or after infection[21].

Live *Giardia* can be identified in humans by the presence of the parasite or parasitic cyst in stool.

2.2 Giardiasis Treatment

There is currently no effective and approved available human vaccine against *Giardiasis* that is available, and with the increase in antibiotic resistance around the world, the requirement for new therapies to treat *Giardiasis* has come into focus[22].

Traditional pharmacological treatments include 5-Nitromidazoles (e.g. tinidazole, metronidazole), 5-Nitrothiazoles (e.g. nitazoxanide), 5-Nitrofurans (e.g. furazolidone), Aminoglycosides (e.g. paromomycin), Benzimidazoles (e.g. albendazole), Acridins (e.g. quinacrine), and Quinolines (e.g. chloroquine)[22–25]. The mechanism of action is different between drugs, with 5-Nitro based drugs adducting and causing protein/DNA inactivation, whereas acridins can inhibit DNA synthesis, benzimidazoles can interfere with the cytoskeleton, and quinolines/aminoglycosides being unknown[24]. Drugs to treat *Giardiasis* can come with side affects such as gastrointestinal upset, diarrhea, abdominal discomfort, metallic taste, nausea, and vomiting[22–24]. Treatment of symptoms is the most common course of action, which include rehydration (oral or intravenous), and anti-diarrheal medications.

Some non-drug-based methods for the treatment of *Giardiasis* include probiotics, sometimes in tandem with antigiardial pharmacotherapy. In a gerbil model, the use of probiotics reduced the number of cysts in stool[22].

High throughput screening assays are working to identify next generation antigiardial drugs, with modifications to accommodate for the microaerophilic/anaerobic conditions necessary for *Giardia* growth[22]. Hybrid (chimeric) molecules combining functional components of two active molecules is a potential for drug design. Drug repurposing of an already approved drug is another route. Auranofin, an FDA approved drug for the treatment of rheumatoid arthritis, Fumagillin, an EMA antibiotic for the

treatment of microsporidian infections, disulfiram, an FDA approved anti-alcohol dependence treatment drug, and omeprazole (and closely related proton pump inhibitor family compounds), approved for the treatment of gastrointestinal tract acid-related diseases, are some of the pharmacological medications used in the treatment of other conditions that are currently being explored for their efficacy against *Giardia*[22,25]. Well designed clinical trials are needed for new or repurposed drug options to become commonplace in treating *Giardiasis*.

2.3 Giardia Life Cycle

The life cycle of *Giardia* occurs in two main stages; a proliferating trophozoite followed by the infectious cyst[8,16–18]. The trophozoite cytoskeleton is usually around 9.5 to 21μm long and 5 to 15μm wide, pear shaped, motile, and propels itself by means of four sets of flagella that can each behave differently to allow for movement[14–16]. The motion of Giardia trophozoites has been described as "falling leaf motility", as they tumble erradically[14,15]. Trophozoites are most commonly found in liquid or soft stools from infected individuals[14].

The cyst produced by *G. duodenalis* is the stage in life cycle at which the parasite is the most environmentally robust. Infection begins at this stage when a susceptible host ingests a cyst. They are oval in shape, with tough two-layered cyst walls, and four nuclei that are typically situated at one end[14,15]. The cysts are usually 5 to 12μm in length by 7 to 10μm in width[14,15,17,18]. The species lacks several typically found parasitic organelles but has identifiable and unique curved median bodies that can be seen at different stages in the parasite's life cycle[14,15,20]. Infective, highly resistant cysts are more commonly found, in many types of stool[14,15].

After passing through the acidic stomach region, with an increase in environmental alkalinity of the duodenum, two excyzoites are promoted to emerge from the cyst, which then quickly transform into trophozoites[14–16,18]. It is at this stage that the trophozoites attach to the epithelium of the host. The two daughter trophozoites will then replicate asexually by binary fission, which is completed along the longitudinal plane[14,15]. Some of the trophozoites will then undergo encystation, while others continue to replicate, which begins shortly after infection, with the peak rate occurring at one week[15]. A change in environment triggers encystation, which will enable the parasite to survive outside of host organisms[16].

2.4 Cryptosporidium and Cryptosporidiosis

Cryptosporidium has seven species that can infect humans, but there are two species (*Cryptosporidium hominis* and *Cryptosporidium parvum*, which are structurally indistinguishable) that are more commonly associated with the human disease *Cryptosporidiosis*, comprising more than 90% of cases[8,10,11,13,17,26]. The coccidian parasite has been reported as infectious to humans as well as other mammals, reptiles, birds, amphibians, and fish[8,10,11,17,26]. *Cryptosporidium* outbreaks have occurred worldwide, in both developing and developed nations, which has led to the classification of the parasite as the second most found diarrheal pathogen (after rotavirus), causing 12% of total diarrheal deaths in 2015[9].

Characteristic symptoms of *Cryptosporidiosis* include watery diarrhea and abdominal pain, but can also include nausea, vomiting, joint and eye pain, recurrent headaches, dizziness, fatigue, and low-grade fever[8,9,12]. Depending on the host factors (i.e. immune status, age, and exposure frequency), the severity of infection can vary from asymptomatic to life-threatening[8,12]. In immunocompromised individuals, such as patients with AIDS, the percentage of critical cases is increased, with persevering and unrelenting symptoms resulting in severe dehydration, leading to wasting, and significant mortality rates[8–10,12].The prevalence of *Cryptosporidium* as a contributor to worldwide gastrointestinal illness in adults and children makes it a topic of study in water quality.

2.5 Cryptosporidiosis Treatment

Limited treatment options are available for *Cryptosporidiosis*. The only FDA approved treatment, which is a drug that overlaps with the treatment of *Giardiasis*, is nitazoxanide, but has limited efficacy in certain populations, such as children (and is not approved for children under the age of 12 months)[27,28]. There is no available human vaccine for the prevention of *Cryptosporidiosis*.

There are other available pharmacological alternatives for *Cryptosporidiosis* treatment, which are not approved by the FDA, and include paromomycin, azithromycin, and fluoroquinolone[28]. Treatment of symptoms, such as rehydration and anti-diarrheal medications, is the most common option.

Several candidates for *Cryptosporidiosis* therapeutics have emerged during the 2010s, whether it be new drug discovery or repurposing previously approved drugs. Clofazimine, KDU731, BKI-(1294, 1517, 1369, 1534, and 1649), P131, AN7973, Compound 2093, MMV665917, Compound 5, BRD7929, N-methyl-piperazine-Phe-homo-Phe-vinylsulfonephenyl (K11777), P+OIPC, atorvastatin with/without nitazoxanide or itavastatin, Triascin C, acetylspiramycin, and garlicin are some of the candidates that

are currently being screened for efficacy in *Cryptosporidiosis* treatment[27,28]. Most of the above listed compounds are in the discovery phase, but BKI-1708 and KDU731 are in preclinical, while Clofazimine is in clinical[27]. Further studies are required for drugs to become approved as treatment options.

2.6 Cryptosporidium Life Cycle

The *Cryptosporidium* life cycle is complex, with both sexual and asexual reproductive stages; there are six major developmental stages that the parasite undergoes [10,12]. Infection begins when a susceptible host ingests or inhales a thick-walled oocyst. In the lumen of the intestine, four infective sporozoites will be released to bind with the host and develop into trophozoites. The sporozoites are spindle-shaped, move by helical and circular gliding movement, trophozoites are around 1.5 to 2.5μm in diameter. Excystation has been reported to be triggered as a result of a multitude of factors such as carbon dioxide, pancreatic enzymes, and salt content[12]. In the next step, a type I Meront will be formed, which releases merozoites to infect adjacent cells and form either additional type I Meronts or type II Meronts [10,12]. The production of Meronts is a type of asexual fission. The type II Meronts then enter host cells and begin the sexual stage formation of microgamonts and macrogamonts, most of which will develop into thick-walled oocysts to be released into the environment to infect a new host, but thin-walled oocysts can be produced for autoinfection [10,12]. The act of autoinfection is a quality that *Cryptosporidium* possesses that many other parasites belonging to the *Coccidia* subclass do not[12].

The fully sporulated thick-walled cyst is typically within 4 to 6μm in diameter[10,11,17,26]. The oocyst is highly environmentally resistant with wall proteins contributing to the resistance capability[10,29].

2.7 Transmission of Parasites

Transmission methods for both *Cryptosporidium* and *Giardia* occur in similar ways; each organism has a highly infective cystic stage. The method of transmission is through direct contact with contaminated food/water/soil, fecal/genital-oral, untreated and recreational waters, contact with infected animals, person to person contact, or through aerosolized droplets, with the most recognized method of transmission is through contaminated water and food [8–18,21,25,26,30–45]. The lowest infectious dose for *Cryptosporidium* is 1 to 5 oocysts, while for *Giardia* it is as low as 10 cysts, making these parasites especially dangerous for the human population[8,17].

Highly environmentally robust (oo)cysts allow for transmission of the disease to occur widely; when a host organism consumes a(n) (oo)cyst, the parasite will replicate inside of the host to produce more highly infectious (oo)cysts. Those resistant (oo)cysts will either auto-reinfect or be expelled into the environment. In the latter case the (oo)cyst wall enables the organism to survive for several months in the right conditions (ie. cool and damp)[11,14,16,26,38,39,46–48]. A study regarding survival conditions of *Giardia* cysts and *Cryptosporidium* oocysts found that *Giardia* cysts were detected and proved animal infective after 9 weeks of incubation at 4^{o}C in water, soil, and faeces; *Cryptosporidium* oocysts in the same conditions were found to have reduced in number but remained infective for greater than 12 weeks[38]. The same study showed that 2-week incubation of (oo)cysts at 25^{o}C, *Giardia* cysts were not infective after the 2 weeks, while *Cryptosporidium* oocysts were infective, but for a shorter period, and were degraded more rapidly when compared to lower temperatures.

2.7.1 Transmission by Water

One major driving force of contamination is by water. Major routes of exposure can include untreated recreational waters (e.g. water parks, swimming pools, fountains and displays), naturally occurring sources (e.g. rivers and lakes), and contaminated drinking water. Due to (oo)cyst size and increased environmentally resistant viability time, water currents can carry (oo)cysts across varying distances, which can cause outbreaks at locations far from the origin. (Oo)cysts can be found in both surface water and sedimentation, which can affect the treatment process for drinking and recreational water, as well as testing parameters.

Ingestion of (oo)cysts from water is primarily caused by the consumption of contaminated drinking water. Contact with contaminated wastewater, un-composted sewage sludge, or agricultural runoff with manure fertilizers are some of the ways which drinking water may become a vessel for parasites. One of the largest outbreaks of waterborne disease occurred in 1993 in Milwaukee (USA), with the consumption of oocyst-contaminated drinking water, and resulted in an estimated 403 000 individuals being infected[10,17]. Unfiltered surface waters and groundwater wells may both contain (oo)cysts, so long as the conditions are acceptable for viability. *Giardia* cysts are less likely to survive in untreated water when compared to *Cryptosporidium* (in particular, *C. parvum*), however they are typically more abundant in drinking water[8,17].

According to the World Health Organization in 2019, there are at least 2 billion people around the world who use a drinking water source that has been contaminated with faeces[33]. *Cryptosporidium* and *Giardia* are the most common parasites that are reported in wastewater, with (oo)cyst numbers correlating to the infection rates of humans served,

with influence from wild and domesticated animals[33]. Animals and humans that have been infected may produce and pass up to 10 million *Giardia* cysts and 10 billion *Cryptosporidium* per one gram of faeces[38].

Many municipal water utilities test drinking water for cyst contamination, but there is also the infection route of swallowing water while swimming in recreational fresh water or recirculated water. In particular, Giardiasis is sometimes referred to as "beaver fever" particularly in North America, which comes from the epidemiological characterizations of beaver isolates from contaminated recreational and drinking water sources[8,19,49]. Since a host can pass very large numbers of transmissive cysts, it may only take one or a few animals or humans to contaminate a large body or source of water.

2.7.2 Zoonotic Transmission

Zoonotic transmission of both *Cryptosporidium* and *Giardia* is also of major concern as a method of disease migration. Wild and farm animals are susceptible to contaminated drinking water, which may lead to hosting replicating organisms. Veterinary students, researchers who work with animals, farm workers, and children visiting farms are all at risk when encountering animals infected with a strain of parasite with diverse host populations[12,15].

2.7.3 Transmission by Food.

With global transport of many foodstuffs, there is a risk of contamination and migration of foodborne zoonotic pathogens. There are fewer documented foodborne outbreaks when compared to waterborne outbreaks, which is likely due to the lack of investigative tools and the fact that food is transported globally, meaning cases can be difficult to track and correlate[31]. Since food typically is chilled when transported, refrigeration increases the likelihood of survival for cysts during transport. In a study from 2017, it was shown that when lettuce was stored at room temperature, ~50% of surface *Cryptosporidium* and *Giardia* (oo)cysts lost viability within the first 24h of increased temperature exposure[18]. *Giardia duodenalis* alone is estimated to cause around 28.2 million cases of gastrointestinal diarrhea each year resulting from contamination of food[18]. *Giardia* cysts have been detected on many different types of food such as meat, shellfish, fruits, vegetables, and dairy products, with the highest contamination rates on vegetables due to raw consumption[18,31]. One way to reduce food related contamination is by washing fruits and vegetables before consumption, but then comes in the question of the source of water also being contaminated, as well as how the parasites can contaminate food not only as a surface contaminant but also from within the food matrix[31].

Cryptosporidium oocysts are smaller than cysts from *Giardia*, which allows them to be trapped in smaller pores on food. There are currently few standardized methods for the detection of the highly transmissive stages of protozoan parasites regarding food, despite the potential for high numbers of infection[34].

Table 1. Species of *Cryptosporidium* and *Giardia* and their primary infectivity targets.

Cryptosporidium			***Giardia***		
Species	Major host(s)	References	Species	Major host(s)	References
C. hominis	Humans, monkeys	[8,10–12,17,26,31,34]	*G. duodenalis* – *A assemblage*	Humans, livestock	[8,15,17–19,34,49]
C. parvum	Cattle, humans	[8,10–12,17,26,31,34]	*G. duodenalis* – *B assemblage*	Humans	[8,15,17–19,49]
C. muris	Rodents, farm animals, humans	[8,10–12,17,26,31,34]	*G. duodenalis* – *C assemblage (G. canis)*	Dogs	[8,15,17–19,49]
C. suis	Livestock, humans	[8,10–12,17,26,31,34]	*G. duodenalis* – *E assemblage (G. bovis)*	Cattle, hoofed livestock	[8,15,17–19,49]
C. andersoni	Livestock, humans	[8,10–12,17,26,31,34]	*G. duodenalis* – *F assemblage (G. cati)*	Cats	[8,15,17–19,49]
C. wrairi	Guinea pigs, humans	[8,10–12,17,26,31,34]	*G. duodenalis* – *G assemblage (G. simondi)*	Rats	[8,15,17–19,49]
C. canis	Dogs, humans	[8,10–12,17,26,31,34]			
C. felis	Cats, humans	[8,10–12,17,26,31,34]			
C. meleagridis	Birds, humans	[8,10–12,17,26,31,34]			
C. serpentis	Lizards, snakes	[8,11,31]			

1.8 Detection of (Oo)cysts

There are many methods of detecting and characterizing (oo)cysts in a sample. The most popular categories of detection are microscopy based, cytometry based, immunological based, and molecular based. Most detection methods require the cyst to be in liquid media, which then requires filtration, separation, and concentration to determine

which organisms and species are present in a sample. Each sample has some advantages and disadvantages, but debris and other organisms can complicate detection methods by physically, biologically, or chemically interfering with virtually any parasite containing sample.

Filtration methods are commonly used as the first step in (oo)cyst detection methods. Membrane, cartridge, and fibre filtration methods are some of the types of physical filters that are used as precursors to detection of (oo)cysts.

Immunomagnetic separation is a common laboratory tool used for the isolation of targets for further testing. Magnetic beads containing antibodies for the target molecule are incubated with a solution, separated from the sample, washed, and eluted to obtain targets. This method is used frequently in the purification of (oo)cysts and can be combined with other procedures, such as pH relations or turbidity, to isolate targets[35].

Density gradient separation techniques are another category of separation techniques which are commonly used to isolate (oo)cysts. Processes may involve chemicals, such as sucrose, zinc sulfate, or magnesium sulfate, which lead to flotation separation, or centrifugation. Both categories of density gradients can be problematic when concerning viability of (oo)cysts, as they can chemically inactivate or physically destroy delicate matter.

2.8.1 Microscopy Based Detection

Microscopy based methods were some of the first methods employed to detect live parasites and (oo)cysts, with Antoine van Leeuwenhoek in 1681 first physically describing *Giardia* upon finding organisms in his own sample of stool[14,15]. Microscopy can be used to detect samples in water, faeces, tissue, food, and on/in other media. Initial methods using microscopy were based on the adherence of (oo)cysts to a coverslip, following zinc sulfate flotation, and were imaged on a microscope using white light[30,50]. Improvements have been made to microscopic methods of detection, including the addition of chemical stains and dyes (such as Auramine Phenol, Acid Fast stain, and Giemsa), implementation of alternative illumination mechanisms (such as phase contrast and differential interference contrast), and use of more powerful microscopes (such as electron microscopy).

Stains and dyes allow for target organisms to be easily identifiable against a white microscopy background as well as against other organisms in a sample. Environmental samples of water are subject to conditions that may affect a stain or dye’s ability to effectively stain an (oo)cyst.

In a 1989 study published by Cambridge University Press, the conventional methods of staining were compared on *Cryptosporidium* oocysts in both seeded and waterborne outbreak water settings[51]. The stains used were Ziehl-Neelsen (ZN), auramine-phenol (AP), Wright-Giesma (GDQ), safranin-methylene blue (SMB), and FITC-labelled monoclonal antibody (Mab). In raw water from seeded samples, ZN resulted in the oocysts becoming easily identifiable, AP had the same result, but organisms of similar size also fluoresced, GDQ found oocysts difficult to identify, SMB had other organisms take up stain, and Mab had variable fluorescence. In filtered water from seeded samples all stains provided easily identifiable oocysts. When aluminum hydroxide flocculate and rapid sand backflush sediment samples were tested, interference made oocysts more difficult to identify for all stains. In the waterborne outbreak samples of raw and final water, oocysts were detectable with each stain. However, AP, GDQ, SMB, and Mab had some confusion with other organisms of similar shape in size in raw water.

Even with the addition of stains and dyes, (oo)cysts can sometimes be difficult to identify in a sample, especially if the sample is non-filtered. Utilizing different light sources, such as phase contrast (PC) and differential interference contrast (DIC) can aid further in identifying (oo)cysts in a transparent, unstained sample, eliminating the need for chemicals and staining protocols before visualization.

PC employs a mechanism of light delivery that utilizes the variations in phase of a transparent organism, that correspond to changes of light wave amplitude. Since the human eye is only sensitive to amplitude and wavelength of light, phase information is rendered invisible without special equipment that separates background light from specimen scattered light. Constructive interference between scattered and background light makes identifiable features in the parasites and (oo)cysts more visible. Contrast is improved by using the combination of a condenser and a phase shift ring to separate specimen light from the background light, which changes with correspondence to the minute refractive index differences between intra and extra cellular components. This method has the tendency to produce a diffraction halo surrounding the specimen.

DIC is another method of microscopy that can aid in visualizing transparent samples, which also employs phase changes of light. Instead of using a condenser, DIC utilises polarizing filters and Wollaston Prisms to segment the light into orthogonal components. This method also improves contrast between the specimen and the background and is based on the optical path length and optical density variations of the sample. The image has the appearance of a three-dimensional object and reduces the diffraction halo seen in PC. In detecting *Cryptosporidium* and *Giardia*, DIC provides morphology information that allows for the distinction from autofluorescent algae[52].

Scanning electron microscopy (SEM) is a method that has been used to visualize both *Cryptosporidium* and *Giardia*[53,54]. SEM is completed by scanning the surface of a target with a focussed beam of electrons, which interact with the atoms in the target to produce a signal which gives topographical and compositional data about the target. This branch of microscopy requires a highly specialized and expensive microscope, and is more used in characterization rather than detection.

Detection of organisms using holographic microscopy have been demonstrated in the use of detecting waterborne parasites[46,55,56] . Using partially coherent spatial illumination, automated detection and classification of *G. lamblia* was implemented in drinking water based on textural features from optical phase (instead of morphological features)[55]. This was completed by the computation of propagating matrices which identify the three-dimensional position of an organism. A different method of this has been demonstrated with a lensfree approach, making the microscope more compact, lighter and increases the field of view. [56]

In more recent years, the development of cost-effective, portable, lensfree microscopy methods have been developed, some with added deep learning-enabled label-free detection methods[46,56]. Using colour, lens-free, holographic imaging, with pulsed illumination, the trained convolutional neural network cytometer captures and reconstructs phase intensity images of targets within a constantly flowing sample[46]. This method has been used to identify *G. lamblia* cysts in low concentration (<10 cysts per 50mL) in real time[46]. This method is attractive due to its field-portable and low-cost nature, especially for remote and resource limited locations.

Microfluidic chips are another emerging platform for microscopy-based detection. With the use of a y-channel, waveguides, immersion oil, and the analysis of Mie scattering, detection of pre-treated, inactivated *C. parvum* oocysts was demonstrated[57]. This method required pre-treatment of samples, which can be an unideal scenario in point-of-care uses but did not require substantial labour or technician training. For near-real time detection, the method had a limit of detection of 1-10 oocysts/mL but can be combined with pre-filtration or concentration to increase the limit. This method is attractive for its field portability, however it needs to remove the reliance on pre-treatment to become commonly used method in field.

Increased accessibility of (oo)cyst detection has been established with the development of a smartphone based microscopic method[58]. With the use of a ball lens, (oo)cysts of *Cryptosporidium* and *Giardia* were identified and counted manually on the basis of shape, size, and contrast, with increased contrast via the use of a stain. This method currently relies on manual counting, which can be time consuming and labour intensive, but can be completed by anyone with access to a smartphone and a ball lens.

Microscopy is the first method that was developed for the identification of (oo)cysts and is still a primary detection method that is used today. While adjustments to microscopy can aid in correctly identifying (oo)cysts in a sample, they generally require specific chemicals or lab infrastructure to complete, which can make the process of identification time consuming, labour intensive, and costly. These methods are best suited for wet samples, which is disadvantageous for solid samples such as in food contamination testing. In more recent years, low-cost, point-of-care microscopy-based identification methods have become an attractive alternative to traditional lab microscopy, which can reduce time, costs, and labour, especially when concerned with remote testing locations.

2.8.2 Immunological Based Detection

A subset of microscopy-based detection mechanisms is through immunological labelling utilize antibody-antigen interactions, or other intracellular sites, to label (oo)cysts, which can then be visualized using fluorescence microscopy.

Direct and indirect immunofluorescence assays use a similar principle of dye-conjugated antibodies to detect a(n) (oo)cyst. DIFA stains a target protein directly, offering a higher sensitivity when compared to IIFA, which first binds a primary antibody to a target then uses a dye-conjugated secondary antibody to detect the primary antibody. When using monoclonal antibodies in DIFA, only one antibody may bind to a target antigen, but with IIFA, multiple secondary antibodies can bind to each primary antibody. IIFA offers the advantage over DIFA in this case, as more dye molecules can be associated with the target protein. IIFA requires a longer process of sequential staining when compared to DIFA, which can stain a sample with multiple primary antibodies simultaneously. The antibody in commercially available DIFA and IIFA binds to an epitope that is present on the (oo)cyst wall, which can make the viability of (oo)cysts indistinguishable, since it can bind to empty or sporozoite rich (oo)cysts[59]. Microscopic observation in conjunction with the assay can determine whether an observed (oo)cyst contains sporozoites; the light scattering pattern of full versus empty (oo)cysts is different, which makes them identifiable.

Immunochromatography is of the same principle as DIFA and IIFA but is simplified to an immunochromatography card that uses coloured banding patterns to identify the presence or absence of a target antigen. Similar to a Hematrace or COVID-19 rapid test, two strips of immobilized antibodies are placed on a sample card, with one being a control and the other being a specific antibody for the target of interest. The detection of the targeted antigen is read as present or not present; it is a qualitative measurement.

One water monitoring method that is growing in popularity is enzyme-linked immunosorbent assay (ELISA). ELISA uses an antibody which is linked to a reporter enzyme, whose activity can be measured via incubation with an appropriate substrate[60]. ELISA is useful for identifying a target protein in a complex mixture, even within a crude preparation, by immobilizing reactants to a microplate, making it easier to separate bound material from unbound material. ELISA can be used with direct assay, indirect assay, and sandwich techniques. Direct and indirect methods are the same as described in DIFA and IIFA, while sandwich uses a capture antibody (with at least two antigenic sites) pre-coated to the microplate as well as a detection antibody. The sandwich method, deemed as such since antigens are sandwiched between two layers of antibodies, removes the filtration and purification steps performed prior to the assay and enhances sensitivity of the assay. The detection method can be semiquantitative, quantitative, or qualitative, based on whether the colourmetric data is graphed or simply compared. Due to the use of an enzyme, the results have a short window of time in which they can be read.

Enzyme-linked immune-culture assay (ECLIA) has the same logistical methods as ELISA, with the addition of a coupled Sulfo-Tag as the reporter molecule and a specific substrate for the Sulfo-Tag[61]. ECLIA also has specialized plates, which are inserted into a reader that produces an electric pulse. The electric pulse initiates the conversion of the substrate, which in turn produces chemiluminescence. The chemiluminescence data can then be compared or graphed, meaning it could be interpreted as semiquantitative, quantitative, or qualitative. One advantage that ECLIA has over ELISA is that the substrate is activated by the electric pulse, eliminating the result timing associated with the simple enzyme usage in ELISA.

Fluorescence in-situ hybridization (FISH) differs from the above methods of labelling by targeting chromosomal locations within the nucleus of an organism, with fluorescent DNA probes[59,62]. It is a cytogenetic technique that does not require cell culturing to complete. Typically, FISH is used in disease screening, and has applications in personalized medicine, but it can also be used in (oo)cysts detection. The technique utilizes a labelled section of DNA that has a target site within the organism of interest, which then binds to the target and produces fluorescence immediately if labelled directly or waits for an immunological or enzymatic initiated fluorescence if labelled indirectly. The process of FISH can be time consuming and labour intensive but can be completed with multiple distinct fluorochromes simultaneously to detect multiple locations within the DNA. FISH data can be semiquantitative, quantitative, or qualitative.

FITC, or Fluorescein-5-isothiocyanate, is a xanthene dye that labels proteins that can be visualized by microscopy and cytometry, can be used in immunocytochemistry, and has a range of other applications. FITC is the most widely used fluorescence labelling reagent; labelled antibodies, proteins, and substrates can be used to measure a variety of

cell types and processes[63]. It is known for having a high quantum efficiency and conjugate stability. High protein concentrations, or precipitation or aggregation of proteins, can lead to the failure of this method, as well as the failure to remove unreacted FITC which can lead to high background fluorescence in visualization. Modifications in the typical protocol (such as tandem affinity purification or TAP) can reduce the probability of error and low-quality visualization[63]. This method can be time consuming but is seen as a relatively straightforward method of fluorescence staining. In the context of (oo)cyst identification, this method has been used to stain monoclonal antibodies to visualize in microscopy[51].

The use of aptamer technology has been recently demonstrated a detection method for *C. parvum* oocysts[64]. An aptamer is a designable synthetic biomolecule, composed of a single stranded DNA or RNA oligonucleotide, which binds with its target with high affinity and selectivity, by a process of unique three-dimensional interactions[65]. Electrochemical aptasensors have been developed as able to distinguish between *C. parvum* and *G. duodenalis* for the detection of (oo)cysts in the context of both fresh produce and drinking and recreational water sources[64,66]. The aptamers synthesized have additional functional groups on sites that do not disrupt their structure or function and have the potential to be conjugated to magnetic beads for the concentration of (oo)cysts to a smaller volume sample[65]. Aptamers are immobilized to a surface, and the binding of *C. parvum* oocysts to the aptasensor causes an increase in the redox current of the device, which can then be measured by square wave voltammetry[64,66]. One concern as to the implementation of aptasensors in water quality monitoring is the time and labour intensive processes associated with the generation of aptasensors, the rapid degradation of aptamers by the means of nucleases, and cross-reactivity[65].

Recent advances in CRISPR/Cas technology have been used in immunosensing *C. parvum* oocysts by the means of combining antibody-based immuno-recognition combined with CRISPR/Cas12a fluorescent signal amplification by the means of a hybrid antibody-DNA conjugate and uses a conventional ELISA setup[67]. The *Cryptosporidium* oocyst acts as the analyte in which a sandwich method of detection is realized. Utilizing 4 different matrices to represent different environmental testing environments (yogurt, orange juice, lite milk, and dirt suspension), results indicated satisfactory fluorescent selectivity and signal intensities[67]. Costs associated with this method can be high, but it is a highly specific assay, and it has a short runtime. Further improvement of this system would be to implement it on removable devices.

Most immunological based methods of visualization require pre-filtration and concentration of samples to stain targets of interest more effectively. Experiments involving these methods of staining can be completed on liquid samples, or filters that liquid samples have been run through, which can make it difficult to analyze solid

samples such as food. Every staining protocol requires the use of specialized lab infrastructure in the form of a fluorescence capable microscope, and specific chemicals to stain, dye, or label a target of interest. Environmental samples can contain inert particles or algal cells that exhibit strong autofluorescence, or posses similar light scattering characteristics to labelled (oo)cysts, which poses an obstacle to using fluorescence-based detection methods. Certain stains and dyes are susceptible to photobleaching and photodegradation, meaning high chemical turnover rates and increased costs. In these ways, it can make this visualization techniques less accessible to people or populations that lack resources and equipment, due to budgetary reasons or remote locations.

2.8.3 Cytometry Based Detection

Cytometry is a commonly used method for the sorting or counting of cells, which typically have been pre-labeled with fluorescent markers. Cells contained in a buffer solution are inserted into a chamber, which then ideally carries the cells through a flow cell or detection window one cell at a time. The detection window is where the cells are exposed to a laser which produces a fluorescence response in labeled cells, or where data from light scattered can be characteristic to the components of the cell. The data collected is from different detection channels that are connected to a computer and can provide the number of instances that a certain characteristic is observed; the obtained data is quantitative.

Cytometry is an alternative to microscopy when concerned with the number of times a target within a cell can be observed, rather than the spatial location of a target within a cell. With terms of detecting (oo)cysts, different forms of cytometry can be used such as time-gated flow cytometry[50,68], fluorescence activated cell sorting (FACS)[50,69], immune-dot blot assays[50,70], and laser-scanning cytometry (LSC)[50,52].

Time-gated flow cytometry is used to in the detection of long-lifetime luminescence (>1 microsecond) in labeled targets, based on temporal-domain discrimination[68,71]. This concept was demonstrated with in a 2009 experiment published in SPIE, where FITC, fluorochromes CY3, phycoerythin (PE) and tetramethylrhodamine B thioisocyanate (TRITC) antibody labelled *Giardia lamblia* cysts and a UV LED were used in a time-gated flow cytometer but failed to detect at a rate higher than ~13% successful due to the low excitation efficiency[68]. Time-gated flow cytometry has the potential to be further improved to detect labelled cysts; with a coherent light source or high-powered UV LEDs, the detection rate is expected to improve for labelled (oo)cyst detection.

FACS utilizes the same principles as typical flow cytometry, but physically sorts mixtures of heterogenous cell samples rather than simply collecting data on them. FACS

was successfully demonstrated to recover *Cryptosporidium* and *Giardia* (oo)cysts from river and reservoir water samples in excess of 92%, which allowed for further analysis (such as viability testing)[69]. This method is attractive as a method to sort (oo)cysts that are going to be further explored by microscopy, immunological testing, or molecular based testing, since it has a higher recovery rate than other methods such as density gradient centrifugation. (Oo)cysts that are attached to particulate matter can be detected and sorted, and this method preserves older (oo)cysts, like ones that are commonly found in environmental samples.

Quantum Dot immune-dot blot assays use alternatives to organic fluorophores as biological labels, which have been demonstrated to label (oo)cysts successfully but require improvement to become an efficient detection method[70]. Quantum dots (QDs) are inorganic crystalline nanoparticles that have been shown to be superior to conventional fluorophores in photostability, fluorescence intensity, and photobleaching threshold, and have been used to detect *Cryptosporidium* and *Giardia* by epifluorescence microscopy[70,72–74]. QDs are typically bioconjugated semiconductor composites or nanocrystals, have a wide spectrum of excitation wavelengths, and have narrow, symmetrical, and tunable emission spectra[72–74]. The tunable emission is an attractive quality for multiplexing reactions, which could provide quantitative measurement of environmental samples, so long as target organisms have species specific antibodies, detecting multiple organisms simultaneously. QDs can be conjugated with biomolecules using a universal approach, which limits the customized chemistry required for many traditional organic dyes[70,72]. When regarding flow cytometry, (oo)cysts stained with QDs exhibited significantly lower mean fluorescence intensity measurements when compared to organic conjugates, against expectations, as non-specific binding occurred[70]. To implement QD based detection methods in flow cytometry, significant improvements would need to be made to reduce non-specific staining in environmental samples.

LSC is functional improvement to traditional flow cytometry that overcomes many of the limitations of the typical method. LSC can analyze individual cell time-resolved events, such as drug uptake and efflux, it may collect data on morphology and the location of the fluorochrome from within the cell, and it can reanalyze cells subsequently with alternative probes. There are various types of data that can be recorded by LSC for each measured object: integrated fluorescence intensity, maximal pixel intensity within the integration contour area, the xy coordinate of the maximal pixel, integration area, perimeter of integration contour, circularity, fluorescence intensity of a torus of user defined width integrated over a peripheral contour defined area around the integration contour, the time (according to the clock on the measurement computer) at the time of measurement, and FISH measurements[75]. LSC requires specialized equipment to complete, however it compliments typical flow cytometry and offers many advantages. In a Journal of Applied Microbiology study for the detection of *Cryptosporidium* oocysts

and *Giardia* cysts, as an alternative to manual microscopy, LSC immunofluorescence detection was completed on glass slides, confirmed with epifluorescence and DIC, and validated by manual microscopy, and was shown to count (oo)cysts at numbers that were at the least equivalent to manual microscopy[52]. LSC can reduce times compared to manual microscopy and reduces the error associated with operator fatigue and subjectivity but requires that samples be mounted onto a glass slide, which can increase preparation time.

Generally, flow cytometry has the added ability of automation, which improves time and labour-associated drawbacks that other detection methods may suffer from. However, the process has several limitations such as the inability to analyze time-resolved events, morphology, subcellular fluorochrome localization, cell re-analyzation with flow cytometry, samples must be in a liquid buffer, and large sample sizes require pre-concentration[75].

2.8.4 Molecular Based Detection

Molecular methodologies are generally used for the identification of a specific species in a sample. Molecular procedures are an assembly of techniques to identify and analyze biological markers that are within an organism's proteome or genome. Tools based on this principle are used in diagnosing and monitoring disease, treatments for disease, research, prenatal screening, and other specialities including water monitoring for infectious organisms. Target regions of DNA or a target protein are amplified and replicated from a sample with the use of thermocycling, DNA/RNA primers, a polymerase enzyme, a buffer, and stabilizing agents. The amplified product(s) are run through a gel matrix to separate the fragments of DNA or the proteins by length or charge/size, respectively, by applying an electric field to either an agarose gel or polyacrylamide gel. The banding patterns visualized by alternate light source on the gel can give information about the sizes of the fragments of DNA or the proteins, which can provide information about whether a target piece was present in the sample. The separated DNA or proteins can then be sequenced or run through an assay for further analysis.

Polymerase chain reaction (PCR) can be used on its own as a diagnostic method for parasitic oocysts, but it can also be used in combination with immunomagnetic separation to provide higher quality data[76,77]. PCR has the advantages of higher sensitivity, relatively rapid analysis, low cost (in comparison with other methods), tandem detection of multiple pathogens or regions of interest, and discrimination between species/strains[77]. Specific primers corresponding to regions within the genome of *Cryptosporidium* and *Giardia*, which can be further specified to individual species (such

as *C. parvum* and *G. lamblia*), are incubated with purified DNA and a polymerase enzyme, and allowed to undergo thermocycling. The process of thermocycling occurs by heating the sample to denature the DNA, lowering the temperature to allow for primers to anneal to target regions, and then raising the temperature to the ideal for the polymerase enzyme to elongate the newly annealed primer. The product of DNA increases two-fold, so repeating the cycle multiple times can lead to millions of copies of the DNA. Sensitivity from purified samples of (oo)cysts has been found to be higher than environmental samples, due to DNA degradation, inhibition by coextracted materials and non-specific binding and amplification products[77]. This can be overcome by the addition of chemicals (such as BSA) or by adding steps (such as immunomagnetic separation, spin columns, or flow cytometry) to purify a sample before DNA amplification[76,77]. PCR based techniques require pre-concentration of a sample; due to the potentially low content of target DNA in an environmental sample, filtration is commonly used to increase the quantity of usable and amplifiable DNA, as well as decrease the population of amplification inhibitors in the sample[76–83]. Integrating in vitro cell culture into PCR methods has been demonstrated as a method for determining infective (oo)cysts[84,85], since using traditional PCR techniques with no modifications deems it impossible to tell the viability of an (oo)cyst[77,79,80,86]. *Cryptosporidium* wall proteins, such as the COWP gene, and *Giardia* Assemblages A, B, and E specific genes, such as *β-giardin*, are typical targets of PCR quantification.[87]

Nested PCR is an additional step that can be added to a PCR protocol that is designed to improve sensitivity and specificity[76,80,81,88]. The DNA undergoes one round of PCR as per the typical protocol, but for the second round of reaction, a different primer is used, with the likelihood of non-specific targets possessing sites for both primers decreasing the chance of unwanted products. The addition of this step increases the time to detection and requires a second primer, but can be performed on more convoluted samples, such as environmental water samples, with an increased chance of specificity. In a published article in Water Research (2001), it was shown that with a nested PCR could reliably detect as few as 8 *Cryptosporidium* oocysts spiked in water but stated that turbidity and debris in environmental samples still proved a significant problem for PCR inhibition due to the presence of inhibitors that were not washed out[80]. Nested PCR allows for the detection of (oo)cysts that are intact, as well as cost effectiveness, technical simplicity, and the adaptiveness to include enumeration of DNA.

Real-time PCR is a method (also referred to as quantitative PCR or qPCR), is a method of PCR which enumerates amplified DNA in real time rather than at the end of thermocycling. There are two common methods which are utilized in qPCR for enumeration: non-specific DNA intercalating dyes and sequence-specific fluorescence reporter containing oligonucleotide probes which must hybridize with a complementary DNA region to fluoresce. The DNA detected by either of the to common methods are

compared to a standard curve. qPCR has been demonstrated effectively in quantifying DNA from *Cryptosporidium* and *Giardia* (oo)cysts[83,89,90]. This method of detection is attractive due to its real time production of results but is still susceptible to environmental inhibitors and cannot detect viability.

Droplet digital PCR (ddPCR) removes the reliance on a standard or calibration curve by providing the absolute quantitation[91–93]. ddPCR partitions PCR solutions into separate nano-litre sized droplets (on the order of thousands per sample), where separate PCR reactions take place. Partitioning methods can include well plates, capillaries, emulsion oils, or regions of nucleic acid binding surfaces. Each reaction centre is checked for fluorescence after a desired number of amplification cycles and provides a binary readout of fluorescent (1) or non-fluorescent (0), which is recorded as a fraction of fluorescing centres[92]. This method has been conducted to compare against qPCR in detecting *Cryptosporidium*, and was shown to have higher precision than qPCR, but became poorer with a decrease in DNA concentration, and was shown to be less affected by the presence of inhibitors[93]. This method of detection is still unable to distinguish viability in oocysts.

Reverse transcriptase PCR (RT-PCR) has been shown to specifically identify viable oocysts[76,78,80]. This form of PCR is based on the use of RNA as a template, which is reverse transcribed into complimentary DNA (cDNA). The reverse transcriptase enzyme synthesizes a DNA/RNA hybrid, then degrades the RNA portion to give a single stranded cDNA fragment, which is then elongated by DNA polymerase. Once the initial step of RT-PCR is completed, the regular PCR process of repetitive thermocycling amplifies the DNA. RT-PCR has been used in conjunction with other detection methods to provide higher quality data and more sensitive detection methods[77–80,83]. One method described in a paper published in the American Society for Microbiology utilized the detection of mRNA transcripts by RT-PCR in *Cryptosporidium* and *Giardia* (oo)cysts with an induced heat shock protein gene, since the levels of mRNA exhibit rapid decay following cell death[78]. This method was compared with immunofluorescence microscopy (DAPI) and was found to be more sensitive[78]. Immunomagnetic separation has also been used with RT-PCR as a viability assay for *C. parvum* oocysts, which lowered the limit of detection for oocyst spiked concentrated environmental samples of water[79]. This method was unable to detect oocysts if they were inactive, but regular PCR tests completed in tandem confirmed the presence of inactive cysts[79]. Implementing cell culture with traditional PCR, RT-PCR, and immunofluorescence assays have been compared and demonstrated as methods to monitor infectivity of *Cryptosporidium* oocysts, with immunofluorescence assay having the lowest rate of false positives and highest rate of detection[85].

Restriction fragment length polymorphism assay PCR (RFLP-PCR) is another form of PCR that has been used to identify *Cryptosporidium* oocysts in water[50,81,94]. In tandem with nested-PCR, RFLP-PCR can detect low densities of oocysts, as well as identify if the contamination is human-pathogenic in origin[81,94]. This technique utilizes polymorphisms, which are variations in homologous DNA sequences that distinguish individuals, and restriction enzyme sites (specific regions where a restriction enzyme will cleave) to digest DNA into fragments, which are then amplified by PCR. Small-subunit rRNA-based nested RFLP-PCR was shown to amplify DNA from five or fewer oocysts, and identify individual species based on the analysis of restriction enzyme cleaved DNA; incubation of oocysts with specific primer sets to exploit polymorphisms allows for differentiation [81,94].

Loop-mediated isothermal amplification (LAMP) is a relatively new method that amplifies DNA with high specificity and efficiently, at a rapid rate under isothermal conditions, employing a DNA polymerase enzyme in tandem with a set of specially designed primers that locate distinct target DNA sequences, and amplify DNA at a significantly higher rate than PCR[95,96]. At a constant temperature, typically 4 primers amplify 6 regions in a target gene, initiated by an inner primer which possesses sense and anti-sense strands of target DNA, followed by an outer primer, which displaces the DNA synthesis and releases a single-stranded DNA, which serves as a template for DNA synthesis that is primed by the second inner and outer primers, which hybridize to the other end of the target sequence to form a stem and loop structure of DNA[95]. Following rounds of LAMP cycling yield a new stem and loop DNA product which is twice as long as the original stem and loop, as well as the original stem and loop, with repeated cycling producing in excess of 10^9 copies of the target DNA in under an hour, with a final product stem and loop DNA having inverted repeats and broccoli-like structures that have a high selectivity of target sequences[95]. In comparison with PCR, LAMP has been demonstrated as an effective method to detect picograms of *Cryptosporidium* and *G. duodenalis* DNA in a sample[96–100]. RT-LAMP has also been used to detect *Cryptosporidium* oocysts, utilized to decrease the limit of detection of traditional LAMP, and the labour associated with the procedure by making the assay single step[96].LAMP is an attractive DNA amplification method due to its simplicity, rapidity, lack of difficult washing steps, immunity to the presence of inhibitors (that reduce PCR), cost effectiveness, and lack of highly specialized equipment[95–100]. One limitation to LAMP is that it is highly based on primer design, which is limited to the published gene sequences available in databases. There are a limited number of organisms that have been catalogued by individual researchers, and further investigation and research on primer development would be required to allow LAMP to become a more commonly used method of DNA amplification.

A DNA microarray is an assembly of probe DNA sequences attached to a solid surface, used to measure gene expression levels by hybridizing to cDNA or cRNA. Microarrays have been designed and used with probes to specifically detect various species of *Cryptosporidium*[101]. The use of microarrays can be used to detect multiple organisms in a single sample, which has the potential to benefit water quality research. Microarrays require pure genomic DNA, which increases preparation time for samples. The design of DNA probes comes with challenges; optimal probes can be predicted with specialized software, but the performance of probes designed does not always occur as expected in vitro, as well as the decrease in sensitivity when compared to other methods such as PCR[101].

Nucleic acid sequence-based amplification (NASBA), with subsequent electrochemiluminescence detection, has been used in the detection of viable *Cryptosporidium* oocysts from environmental samples[102]. The technique produces multiple copies of single stranded RNA, by means of a two-step process which utilizes primers which anneal to RNA and an enzyme cocktail to amplify the RNA, which can then be used to produce cDNA. Amplification protocols can be isothermal or non-isothermal[95]. In a study published by ACS Publications, a heat shock protein from *Cryptosporidium* was targeted and amplified by NASBA, hybridized with DNA probes, and quantified, to produce a detection limit of around 5 viable oocysts per sample[102]. One limitation of this detection method is its inability to detect non-viable oocysts.

Electrophoretic mutation scanning (EMS) can separate DNA molecules in a manner which is dependent on nucleotide sequence[103]. Heteroduplex analysis is a method which utilized particular electrophoretic conditions to determine if one or more types of a DNA sequence exist in a sample, since under the conditions, heteroduplex molecules containing mismatches can be separated from identical molecules that have no mismatches[103103]. This process has been used in a heteroduplex mobility assay (HMA) for the rapid detection of diversity in the sequences of different *Cryptosporidium* species[104]. These assays can be useful in identifying variations in genotypes within a parasite species, and can help in visualizing the migration of parasites and determining outbreaks associated with a specific variations of species.

Molecular based detection methods display tremendous potential in detecting *Cryptosporidium* and *Giardia* (oo)cysts, but often require the use of specialized equipment, chemicals and agents, filtration methods, and extensive procedures to remove inhibitory factors. Procedures typically need to be transported to a lab facility for testing, which makes water quality monitoring in remote locations and locations with a lack of infrastructure difficult, timely, and costly.

2.8.5 Other Detection Mechanisms

Biofilms are low-cost sample reservoir that can be scraped to determine potential high-risk regions in a watershed that may need further investigation and have been demonstrated to provide data on *Cryptosporidium* oocysts[105]. Traditional methods of sample collection involve the filtration of 10L or more of water. In tandem with methods of immunomagnetic separation and (D or I)IFA, biofilms were analyzed up and downstream of a wastewater treatment plant, and off of submerged rocks or glass and provided information on the presence of oocysts in environmental waters[105].

Electrochemical impedance spectroscopy (EIS) is an electroanalytical method of analysis based on the bio-recognition of events which occur on an electrode surface[106]. It is a steady-state technique that has a wide range of applied frequencies, recognizing small signals for analysis. A non-invasive method of detecting *C. parvum* oocysts real time, with label free analysis, was developed using an interdigitated microelectrode array, utilizing EIS[107]. In the presence of a low conductive buffer, a linear relationship between oocyst concentration and sample conductivity was observed in a microvolume of fluid, caused by oocysts' ion release under hypo-osmotic conditions[107]. The non-invasive nature of this method is attractive when compared to staining or labelling, potential for automation, and rapidity, as well as typical immunomagnetic separation techniques are non-interfering with the impedance-based strategy of EIS[107].

In another form of electrochemical analysis, potentiometric analysis, two electrodes, one for reference and one for indication, are presented in an electrochemical cell, where the difference in potential between the two electrodes provides information about the concentration of the tested sample[106]. In an ELISA-like assay, an antibody-based horseradish peroxidase-label system was deposited on a screen-printed electrode, which was then potentiometrically detected, with the sensitivity of $5x10^2$ *C. parvum* oocysts per 60ml. This method was carried out within 60 minutes, making it time effective, but needs to be further explored for other *Cryptosporidium* species to determine its applicability in water quality monitoring.

Piezoelectric based biosensors are based on a bioconjugated piezoelectric crystal as a sensor, with the change in oscillation due to the binding of an object to the surface of the crystal[108]. An immobilized anti-*Giardia lamblia* piezoelectric-excited millimetre-sized cantilever biosensor has been demonstrated in detecting <10 cysts/mL in three water matrices (buffer, tap, and river) in 15mis, without a preconcentration step[109]. Since the immobilized antibody does not attract the cysts, flow rate was a factor to be considered in this experiment, with the rate being the limiting factor for transport of cysts to the sensor surface. The increase of flow rate leading to increase in rotation of the nonspherical cyst was assumed to enhance exposure to antibody binding sites, and was observed as the method exhibited a higher response at a higher flow rate. To confirm the response of the

sensor was due to the binding of *G. lamblia*, environmental scanning electron microscope images were taken, and confirmed the presence of cysts. The further feasibility of 1 cyst/mL in a 1L sample, at a flow rate of 5mL/min was shown, which could be an improvement to this method that would decrease the time required for analysis.

Capacitive based biosensors operate on the principle of registering changes in dielectric properties, or the thickness of a dielectric layer, when a target binds to the surface of the sensor. By immobilizing antibodies on interdigitated gold electrodes, *Cryptosporidium* detection was detected by measuring the change in capacitive/dielectric properties upon binding[109]. This label free method showed a detection limit of 40 cysts/mm^2, with the potential to improve and extend detection to other biomarkers in environmental samples. This method does not require pre-treatments and can be integrated into microfluidic devices and made to be part of point-of-care devices.

With the use of antibodies, *C. parvum* oocysts were analyzed with an automated evanescent wave biosensor[110]. Waveguides coated with fluorescently tagged capture antibody solutions were excited within the evanescent field, with results showing increased sensitivity for boiled oocysts. The use of fibre optic biosensors needs further development to increase sensitivity, as only the portion of antibodies bound to the oocysts closest to the surface of the biosensor were detected. This method has the potential of automation but needs further research to be implemented for regular use in water quality monitoring.

Surface enhanced Raman spectroscopy (SERS) is a modification made to traditional Raman spectroscopy that enhances Raman scattering by adsorbed molecules on nanostructures, up to the ability to detect single molecules. This technique has been used for the detection of *G. lamblia* cysts in finished drinking water[111]. This detection method utilized a polycarbonate track etched membrane filter to concentrate (PTCE) cysts, with the addition of immunogold labels, which were then quantified with Raman mapping[111]. Out of the three types of membrane filters tested (Anodisc®, silver membrane, and gold coated PTCE), all three demonstrated low fluorescence background, but the gold coated PTCE was found to be the optimal of the three[111]. The ability to detect a single cyst with this method was demonstrated, however it required 4 hours of instrument time for a single 400µm × 400µm map (which is a fraction of the total surface area) and was undetermined as to the map's reusability. This method has the potential for simultaneous detection of multiple pathogens, but also has an increased cost compared to other detection methods.

A biosensor with direct antibody analysis with mixed self-assembled monolayers (SAMs) was developed to be used with surface plasmon resonance (SPR) in the detection of *C. parvum* oocysts[112]. SPR measures the adsorption of a material on a planar metal surface, with resonant oscillation (which is very sensitive to the change in boundary

caused by surface adsorption) in metallic nanoparticles caused by the interaction with incoming light[113]. This flow type, real-time increased sensitivity by the addition of an immunoreaction step and subsequent binding of antibody-oocyst complexes binding to the sensor's surface to measure $1x10^2$ oocysts/mL. The immunoreaction step of this method was <60mins, with the potential of reuse of unbound antibodies and mixed SAMs leading potential research to improve this method.

In a proof-of-concept experiment, metabolomics was used to detect *Cryptosporidium* in its viable/infective form as well as its non-viable irradiated form[114]. Using excreted metabolites from oocysts, chromatographic and mass spectral data was able to identify and quantify amino acids, carbohydrates, fatty acids, and alcohol type compounds to explain differences between viable and non-viable oocysts within a 24h window from when the sample was acquired to the result. This method requires specific equipment and trained individuals to interpret data but has the potential to aid in further research around parasitic cysts and their life cycles.

2.9 Giardia Disinfection

Giardia cysts are resistant to environmental destruction and are insensitive to some forms of chemical destruction[38]. Regarding chlorine disinfection, cysts are relatively resistant, but can be inactivated with 4mg/L of incubation with the chemical after 60min at 5ºC, when the pH levels are between 6-8[48]. At pH 6 and 7, a chlorine concentration of 8mg/L will inactivate cysts when in contact for 10 minutes, with the incubation time rising to 30 minutes at pH 8. At 25ºC and pH 6, cysts will be killed when exposed to 1.5mg/L of chlorine for a period of 10min. For surface disinfection or spill disinfection, 6% H_2O_2 (hydrogen peroxide) can be used.

Physical inactivation of cysts can occur when cysts are exposed to 10 J/m^2 of UV light at 254nm[48,115]. Cysts are susceptible gamma irradiation, and to both boiling and freezing, which is consistent with boiling water advisories across Canada[48]. Cysts are resistant to ozonolysis[48]. Coagulation-flocculation and filtration (traditional or membrane) practices are common methods to remove cysts from drinking and recreational water sources[37].

2.10 Cryptosporidium Disinfection

Cryptosporidium is resistant to most typical disinfectants and chlorination[13,38]. Oocysts are susceptible 20 minutes of exposure to high concentrations of H_2O_2, ethylene oxide, and ozone (>6%), but are resistant to low concentrations of peracetic acid, sodium

hypochlorite, quaternary ammonia compound, phenolic, glutaraldehyde, ortho-phtalaldehyde, and 70% ethanol[47,116].

Physical inactivation of oocysts can be completed by incubation at elevated temperatures (>70^{o}C) of moist heat for around 20min, freezing (-20^{o}C for 24h or -70^{o}C for seconds), desiccation, UV light, and gamma irradiation[47,116]. In concordance with the removal of *Giardia* cysts, *Cryptosporidium* oocysts can be removed from drinking and recreational water sources by coagulation-flocculation and filtration (traditional or membrane)[37].

2.11 (Oo)cyst Handling

Both *Cryptosporidium parvum* and *Giardia lamblia* are Risk Group 2 classifications which require Containment Level 2 facilities for handling[47,48]. Lab coat, gloves, and eye protection must be worn when handling (oo)cysts. Precautions against the production of aerosols must be taken, such as handling the (oo)cysts within a biological safety cabinet (BSC). Specimens must be stored in labelled leak proof containers, and all surfaces and wastes that have made potential contact with the organisms must be disinfected.

2.12 Indigenous Communities and Water

Indigenous communities in Canada live with an increased rate of high-risk drinking water systems and advisories[5,117,118]. Canada has a decentralized approach to governing water, leaving many small and/or rural communities under boiling water advisories, many of which are First Nations[3,5,117]. Water resources, what was once delegated by municipal government (with influence from provincial and federal governments), is now managed by a tri-departmental structure at the federal level, which consists of Aboriginal Affairs, Northern Development Canada, and Health and Environment Canada, which share in the duty of safe delivery of drinking water[3,117,119]. The Truth and Reconciliation Commission, in response to the Indian Residential School Settlement Agreement issued in 2007, began a nationwide discourse on the need to improve Canada's relations with its Indigenous populations, with water resources commanding a forefront in the battle to improve relationships[117,120]. Since 2015, 136 long-term drinking water advisories have been lifted, with 31 still in effect, spanning 27 communities over the provinces Saskatchewan, Manitoba, and Ontario[121].

Indigenous communities hold traditional knowledge (TK) in high regard, and Indigenous Elders and communities have distinctive perspectives on water[117,119]. To most

of the non-Indigenous population, water is seen simply as an essential resource necessary for survival, but to Indigenous communities it is more sacred; in some Indigenous communities, water is a gift from the Creator of Mother Earth and holds high spiritual significance[117,119]. Therefore, it is of utmost importance for Indigenous communities to have access to clean drinking water resources, but also clean water to ensure the biodiversity of their land, ecosystems, and environment, of which relationships that Indigenous nations hold importance to[5,119]. Scientific thinking needs to be considered as a companion to TK to develop environmental mandates; pieces of TK that have been picked out of the vast branch of TK and inserted into environmental mandates[119]. When developing detection mechanisms, considerations of sustainability, maintenance, and long term usage need to be implemented in congruence with TK, such as a small device design as to not impact or displace parts of the environment, or long term devices that require fewer maintenance updates where technicians would be required to come to site. This will be further explored in consultation with TK and Indigenous communities.

2.13 Indigenous Communities and Healthcare

Indigenous communities are at a heightened risk to waterborne infections with a rate of 30% higher than the national average but are also at a higher risk for skin problems, and even birth defects caused by water usage[117]. An Indigenous community in the Canadian Arctic has one of the highest self-reported acute gastrointestinal illness rates, as verified by peer-reviewed literature[118]. The increased risk to illness is in large part due to the poor infrastructure surrounding water delivery and storage. With gastrointestinal illness being the most frequently identified health outcome reported in Indigenous communities, it comes into question the resources available to treat and prevent these illnesses.

Access to emergency care health services in remote communities has been described as “unacceptable” by both service providers and users, and many Indigenous patients have reported discomfort in reporting their health issues for a fear of information being shared, resulting in social exclusion[122,123]. This fear can be amplified by the fact that in these communities, many nurses and physicians are only part time; part time health care providers can mean long turnaround times for diagnosis and treatment[122,123]. Part time hours means that many workers have to limit the time they spend with each patient, which can make a patient feel rushed and forced to omit details of their condition(s), leaving a higher chance for conditions and illnesses to be misreported. Many of the healthcare workers in Indigenous communities are underqualified to take on the full responsibility of duties with which they are given, delaying diagnosis and treatment while they consult with an expert physician within or outside of the community[122]. Furthermore, the devices and medical equipment in these communities is often out of date, in poor

condition, or absent altogether, leaving workers and patients with fewer resources to diagnose and treat[122]. Due to the lack of equipment, patients are frequently referred out to external medical facilities and resources, which can increase expense for travel. Some Indigenous communities in North-Western Ontario do not have access to a permanent road, leaving air travel as the only option for transportation to external medical facilities[122,123].

Not only does water quality come into concern when discussing Indigenous healthcare, but Point-Of-Care (POC) devices used for diagnosis of illnesses have become an attractive, low-cost method that could solve some of the discrepancies in Indigenous healthcare. The use of a POC device would reduce the need for expertly trained individuals required to operate some medical devices. The work presented in this thesis builds towards the ultimate goal of a low-cost, POC device that can be used for water quality monitoring but can be easily adapted into a POC medical diagnostic device.

2.14 Conclusion

Detection of *Cryptosporidium* and *Giardia* has been an ongoing effort for a long time, and as technology develops, new detection mechanisms develop also. Many detection mechanisms require the use of chemicals, expensive lab infrastructure, or a technical staff, which are generally limited in many resource poor settings such as remote and Indigenous communities. There is an urgent need for low-cost, point-of-care detection technologies to address issue of effective water quality monitoring, disease infection prevention, diagnosis, and disease management.

8. Cacciò SM, Thompson RCA, McLauchlin J, Smith H v. Unravelling Cryptosporidium and Giardia epidemiology. *Trends Parasitol*. 2005;21(9):430-437. doi:10.1016/J.PT.2005.06.013

9. Mmbaga BT, Houpt ER. Cryptosporidium and Giardia Infections in Children: A Review. *Pediatr Clin North Am*. 2017;64(4):837-850. doi:10.1016/J.PCL.2017.03.014

10. Leitch GJ, He Q. *Cryptosporidiosis-an Overview*.

11. Sunnotel O, Lowery CJ, Moore JE, et al. (No Title). doi:10.1111/j.1472-765X.2006.01936.x

12. Bouzid M, Hunter PR, Chalmers RM, Tyler KM. Cryptosporidium pathogenicity and virulence. *Clin Microbiol Rev*. 2013;26(1):115-134. doi:10.1128/CMR.00076-12

13. Erbert H, Ont P, Happell YLC, et al. *THE INFECTIVITY OF CRYPTOSPORIDIUM PARVUM IN HEALTHY VOLUNTEERS*. Vol 332.; 1994.

14. Wolfe MS. Giardiasis. 1992;5(1):93-100.

15. Adam RD. Giardia duodenalis: Biology and Pathogenesis. Published online 2021. doi:10.1128/CMR

16. Einarsson E, Ma'ayeh S, Svärd SG. An up-date on Giardia and giardiasis. *Curr Opin Microbiol*. 2016;34:47-52. doi:10.1016/j.mib.2016.07.019

17. Smith H v., Cacciò SM, Tait A, McLauchlin J, Thompson RCA. Tools for investigating the environmental transmission of Cryptosporidium and Giardia infections in humans. *Trends Parasitol*. 2006;22(4):160-167. doi:10.1016/j.pt.2006.02.009

18. Ryan U, Hijjawi N, Feng Y, Xiao L. Giardia: an under-reported foodborne parasite. *Int J Parasitol*. 2019;49(1):1-11. doi:10.1016/j.ijpara.2018.07.003

19. Cai W, Ryan U, Lihua Xiao ·, Feng Y. Zoonotic giardiasis: an update. *Parasitol Res*. 1:3. doi:10.1007/s00436-021-07325-2

20. Piva B, Benchimol M. The median body of Giardia lamblia: An ultrastructural study. *Biol Cell*. 2004;96(9):735-746. doi:10.1016/j.biolcel.2004.05.006

21. Mahdavi J, Motavallihaghi S, Ghasemikhah R. Evaluation of clinical and paraclinical findings in patients with reactive arthritis caused by giardiasis: A systematic review. *Semin Arthritis Rheum*. 2022;57:152094. doi:10.1016/J.SEMARTHRIT.2022.152094

22. Lalle M, Hanevik K. Treatment-refractory giardiasis: Challenges and solutions. *Infect Drug Resist*. 2018;11:1921-1933. doi:10.2147/IDR.S141468

23. Tecon RM. Treatment of giardiasis. *J Am Med Assoc*. 1938;110(22):1853. doi:10.1001/jama.1938.02790220055025

24. Watkins RR, Eckmann L. Treatment of giardiasis: Current status and future directions topical collection on intra-abdominal infections, hepatitis, and gastroenteritis. *Curr Infect Dis Rep*. 2014;16(2). doi:10.1007/s11908-014-0396-y

25. Riches A, Hart CJS, Trenholme KR, Skinner-Adams TS. Anti-Giardia Drug Discovery: Current Status and Gut Feelings. *Cite This: J Med Chem*. 2020;63:13330-13354. doi:10.1021/acs.jmedchem.0c00910

26. Fayer R, Morgan U, Upton SJ. Epidemiology of Cryptosporidium: transmission, detection and identification. *Int J Parasitol*. 2000;30(12-13):1305-1322. doi:10.1016/S0020-7519(00)00135-1

27. Love MS, Choy RKM. Emerging treatment options for cryptosporidiosis. *Curr Opin Infect Dis*. 2021;34(5):455-462. doi:10.1097/QCO.0000000000000761

28. Chavez MA, White AC. Novel treatment strategies and drugs in development for cryptosporidiosis. *Expert Rev Anti Infect Ther*. 2018;16(8):655-661. doi:10.1080/14787210.2018.1500457

29. Templeton TJ, Lancto CA, Vigdorovich V, et al. The Cryptosporidium Oocyst Wall Protein is a Member of a Multigene Family and has a Homolog in Toxoplasma. *Infect Immun*. 2004;72(2):980-987. doi:10.1128/IAI.72.2.980-987.2004

30. Koehler A v., Jex AR, Haydon SR, Stevens MA, Gasser RB. Giardia/giardiasis - A perspective on diagnostic and analytical tools. *Biotechnol Adv*. 2014;32(2):280-289. doi:10.1016/j.biotechadv.2013.10.009

31. Smith H v., Nichols RAB. Cryptosporidium: Detection in water and food. *Exp Parasitol*. 2010;124(1):61-79. doi:10.1016/j.exppara.2009.05.014

32. Ongerth, Jerry; Pecoraro JP. Removing Cryptosporidium. 2017;87(12):83-89.

33. Zahedi A, Monis P, Deere D, Ryan U. Wastewater-based epidemiology—surveillance and early detection of waterborne pathogens with a focus on SARS-CoV-2, Cryptosporidium and Giardia. *Parasitol Res*. 2021;120(12):4167-4188. doi:10.1007/s00436-020-07023-5

34. Xiao L, Feng Y. Molecular epidemiologic tools for waterborne pathogens Cryptosporidium spp. and Giardia duodenalis. *Food Waterborne Parasitol*. 2017;8-9(August):14-32. doi:10.1016/j.fawpar.2017.09.002

35. Hsu BM, Huang C, Pan JR. Filtration behaviors of Giardia and Cryptosporidium - Ionic strength and pH effects. *Water Res*. 2001;35(16):3777-3782. doi:10.1016/S0043-1354(01)00117-8

36. Pickering H, Wu M, Bradley M, Bridle H. Analysis of Giardia lamblia Interactions with Polymer Surfaces Using a Microarray Approach. Published online 2012. doi:10.1021/es203637e

37. Betancourt WQ, Rose JB. Drinking water treatment processes for removal of Cryptosporidium and Giardia. *Vet Parasitol*. 2004;126(1-2):219-234. doi:10.1016/J.VETPAR.2004.09.002

38. Olson ME, Goh J, Phillips M, Guselle N, Mcallister TA. *Giardia Cyst and Cryptosporidium Oocyst Survival in Water, Soil, and Cattle Feces; Giardia Cyst and Cryptosporidium Oocyst Survival in Water, Soil, and Cattle Feces*. doi:10.2134/jeq1999.00472425002800060040x

39. Wallis PM, Erlandsen SL, Isaac-Renton JL, Olson ME, Robertson WJ, van Keulen H. Prevalence of Giardia cysts and Cryptosporidium oocysts and characterization of Giardia spp. isolated from drinking water in Canada. *Appl Environ Microbiol*. 1996;62(8):2789-2797. doi:10.1128/aem.62.8.2789-2797.1996

40. Medema GJ, Schets FM, Teunis PFM, Havelaar AH. Sedimentation of free and attached Cryptosporidium oocysts and Giardia cysts in water. *Appl Environ Microbiol*. 1998;64(11):4460-4466. doi:10.1128/aem.64.11.4460-4466.1998

41. Drozd C, Schwartzbrod J. Hydrophobic and electrostatic cell surface properties of Cryptosporidium parvum. *Appl Environ Microbiol*. 1996;62(4):1227-1232. doi:10.1128/aem.62.4.1227-1232.1996

42. Schiperski F, Zirlewagen J, Scheytt T. Transport and Attenuation of Particles of Different Density and Surface Charge: A Karst Aquifer Field Study. Published online 2016. doi:10.1021/acs.est.6b00335

43. Ruohola AMJ, Considine RF, Dixon DR, Fong C, Drummond CJ. Mapping the nano-scale interaction between bio-colloidal Giardia lamblia cysts and silica. doi:10.1039/c2sm25595b

44. Dumètre A, Aubert D, Puech PH, Hohweyer J, Azas N, Villena I. Interaction forces drive the environmental transmission of pathogenic protozoa. *Appl Environ Microbiol*. 2012;78(4):905-912. doi:10.1128/AEM.06488-11

45. Dai X, Boll J, Hayes ME, Aston DE. Adhesion of Cryptosporidium parvum and Giardia lamblia to solid surfaces: The role of surface charge and hydrophobicity. *Colloids Surf B Biointerfaces*. 2004;34(4):259-263. doi:10.1016/j.colsurfb.2003.12.016

46. Göröcs Z, Baum D, Song F, et al. Lab on a Chip Label-free detection of Giardia lamblia cysts using a deep learning-enabled portable imaging flow cytometer †. 2020;20:4404. doi:10.1039/d0lc00708k

47. Pathogen Regulation Directorate PHA of Canada. Pathogen Safety Data Sheets: Infectious Substances – Cryptosporidium parvum. Government of Canada. Published 2011. https://www.canada.ca/en/public-health/services/laboratory-biosafety-biosecurity/pathogen-safety-data-sheets-risk-assessment/cryptosporidium-parvum-pathogen-safety-data-sheet.html

48. Canada PHA of. Pathogen Safety Data Sheets: Infectious Substances – Giardia lamblia. Government of Canada. Published 2011. https://www.canada.ca/en/public-health/services/laboratory-biosafety-biosecurity/pathogen-safety-data-sheets-risk-assessment/giardia-lamblia.html

49. Tsui CKM, Miller R, Uyaguari-Diaz M, et al. Beaver Fever: Whole-Genome Characterization of Waterborne Outbreak and Sporadic Isolates To Study the Zoonotic Transmission of Giardiasis. *mSphere*. 2018;3(2). doi:10.1128/msphere.00090-18

50. Efstratiou A, Ongerth J, Karanis P. Evolution of monitoring for Giardia and Cryptosporidium in water. *Water Res*. 2017;123:96-112. doi:10.1016/j.watres.2017.06.042

51. Smith H v, Mcdiarmid A, Smith AL, Hinson AR, Gilmour RA. An analysis of staining methods for the detection of Cryptosporidium spp . oocysts in water-related samples. 1989;(1987):323-327.

52. de Roubin MR, Pharamond JS, Zanelli F, et al. Erratum: Application of laser scanning cytometry followed by epifluorescent and differential interference contrast microscopy for the detection and enumeration of Cryptosporidium and Giardia in raw and potable waters (Journal of Applied Microbiology (2002. *J Appl Microbiol*. 2003;94(1):158. doi:10.1046/j.1365-2672.2003.01846.x

53. Jahnke V. Ultrastructure of Cryptosporidium parvum Ooctsts and Excysting Sporozoites as Revealed by High Resolution Scanning Electron Microscopy. *Arch Otolaryngol*. 1970;91(3):262-265. doi:10.1001/archotol.1970.00770040368008

54. Benchimol M, Piva B, Campanati L, de Souza W. Visualization of the funis of Giardia lamblia by high-resolution field emission scanning electron microscopy - New insights. *J Struct Biol*. 2004;147(2):102-115. doi:10.1016/j.jsb.2004.01.017

55. Mallahi A el, Minetti C, Dubois F. Automated three-dimensional detection and classification of living organisms using digital holographic microscopy with partial spatial coherent source : application to the monitoring of drinking water resources. Published online 2013.

56. Mudanyali O, Oztoprak C, Tseng D, Erlinger A, Ozcan A. Detection of waterborne parasites using field-portable and cost-effective lensfree microscopy. *Lab Chip*. 2010;10(18):2419. doi:10.1039/c004829a

57. Angus S v., Kwon HJ, Yoon JY. Field-deployable and near-real-time optical microfluidic biosensors for single-oocyst-level detection of Cryptosporidium parvum from field water samples. *Journal of Environmental Monitoring*. 2012;14(12):3295-3304. doi:10.1039/c2em30700f

58. Shrestha R, Duwal R, Id SW, Pokhrel S, Id BG. A smartphone microscopic method for simultaneous detection of (oo) cysts of Cryptosporidium and Giardia. Published online 2020:1-19. doi:10.1371/journal.pntd.0008560

59. Taguchi T, Shinozaki Y, Takeyama H, et al. Direct counting of Cryptosporidium parvum oocysts using fluorescence in situ hybridization on a membrane filter. *J Microbiol Methods*. 2006;67(2):373-380. doi:10.1016/j.mimet.2006.04.017

60. Alhajj M FA. Enzyme Linked Immunosorbent Assay. *StatPearls*. Published online 2022. https://www.ncbi.nlm.nih.gov/books/NBK555922/

61. Bolton JS, Chaudhury S, Dutta S, et al. Comparison of ELISA with electro-chemiluminescence technology for the qualitative and quantitative assessment of serological responses to vaccination. *Malar J*. 2020;19(1):1-13. doi:10.1186/s12936-020-03225-5

62. Hu L, Ru K, Zhang L, et al. Fluorescence in situ hybridization (FISH): An increasingly demanded tool for biomarker research and personalized medicine. *Biomark Res*. 2014;2(1):1-13. doi:10.1186/2050-7771-2-3

63. Chaganti LK, Venkatakrishnan N, Bose K. An efficient method for FITC labelling of proteins using tandem affinity purification. *Biosci Rep*. 2018;38(6):1-8. doi:10.1042/BSR20181764

64. Iqbal A, Labib M, Muharemagic D, Sattar S, Dixon BR. Detection of Cryptosporidium parvum Oocysts on Fresh Produce Using DNA Aptamers. Published online 2015:1-13. doi:10.1371/journal.pone.0137455

65. Hassan EM, Örmeci B, Derosa MC, Dixon BR. A review of Cryptosporidium spp. and their detection in water. Published online 2021. doi:10.2166/wst.2020.515

66. Iqbal A, Liu J, Dixon B, Zargar B, Sattar SA. Development and application of DNA-aptamer-coupled magnetic beads and aptasensors for the detection of Cryptosporidium parvum oocysts in drinking and recreational water resources. 2019;857(August):851-857.

67. Li Y, Deng F, Hall T, Vesey G, Goldys EM. CRISPR / Cas12a-powered immunosensor suitable for ultra-sensitive whole Cryptosporidium oocyst detection from water samples using a plate reader. 2021;203(August). doi:10.1016/j.watres.2021.117553

68. Jin D, Piper JA, Leif RC, et al. Time-gated flow cytometry: an ultra-high selectivity method to recover ultra-rare-event μ-targets in high-background biosamples. *J Biomed Opt*. 2009;14(2):024023. doi:10.1117/1.3103770

69. Vesey G, Hutton P, Champion A, et al. Application of flow cytometric methods for the routine detection of Cryptosporidium and Giardia in water. *Cytometry*. 1994;16(1):1-6. doi:10.1002/cyto.990160102

70. Ferrari BC, Bergquist PL. Quantum dots as alternatives to organic fluorophores for Cryptosporidium detection using conventional flow cytometry and specific monoclonal antibodies: Lessons learned. *Cytometry Part A*. 2007;71(4):265-271. doi:10.1002/cyto.a.20381

71. Jin D, Piper JA, Leif RC, et al. Time-gated flow cytometry: an ultra-high selectivity method to recover ultra-rare-event μ-targets in high-background biosamples. *J Biomed Opt*. 2009;14(2):024023. doi:10.1117/1.3103770

72. Zhu L, Ang S, Liu WT. Quantum Dots as a Novel Immunofluorescent Detection System for Cryptosporidium parvum and Giardia lamblia. *Appl Environ Microbiol*. 2004;70(1):597-598. doi:10.1128/AEM.70.1.597-598.2004

73. Lee LY, Ong SL, Hu JY, et al. Use of semiconductor quantum dots for photostable immunofluorescence labeling of Cryptosporidium parvum. *Appl Environ Microbiol*. 2004;70(10):5732-5736. doi:10.1128/AEM.70.10.5732-5736.2004

74. Singh S, Dhawan A, Karhana S, Bhat M, Dinda AK. Quantum dots: An emerging tool for point-of-care testing. *Micromachines (Basel)*. 2020;11(12):1-23. doi:10.3390/mi11121058

75. Masedunskas A, Sramkova M, Parente L, Weigert R. Cell Imaging Techniques. In: Vol 931. Springer Science+Business Media; 2013:153-167. doi:10.1007/978-1-62703-056-4

76. Hallier-soulier S, Guillot E. An immunomagnetic separation polymerase chain reaction assay for rapid and ultra-sensitive detection of Cryptosporidium parvum in drinking water. 1999;176:285-289.

77. Rochelle PA, Leon RDE, Stewart MICH, Wolfe ROYL, Verne L. Comparison of Primers and Optimization of PCR Conditions for Detection of Cryptosporidium parvum and Giardia lamblia in Water. 1997;63(1):106-114.

78. Kaucner C, Stinear T. Sensitive and rapid detection of viable Giardia cysts and Cryptosporidium parvum oocysts in large-volume water samples with wound fiberglass cartridge filters and reverse transcription-PCR. *Appl Environ Microbiol*. 1998;64(5):1743-1749. doi:10.1128/aem.64.5.1743-1749.1998

79. Hallier-soulier S, Guillot E. An immunomagnetic separation – reverse transcription polymerase chain reaction (IMS-RT-PCR) test for sensitive and rapid detection of viable waterborne Cryptosporidium parvum. 2003;5:592-598.

80. Monis, Paul TMonis, P. T., & Saint, C. P. (2001). DEVELOPMENT OF A NESTED-PCR ASSAY FOR THE DETECTION OF CRYPTOSPORIDIUM PAR V UM IN FINISHED WATER. 35(7) 1641–1648., Saint CP. DEVELOPMENT OF A NESTED-PCR ASSAY FOR THE DETECTION OF CRYPTOSPORIDIUM PAR V UM IN FINISHED WATER. 2001;35(7):1641-1648.

81. Nichols RAB, Campbell BM, Smith H v, Al NET, Icrobiol APPLENM. Identification of Cryptosporidium spp . Oocysts in United Kingdom Noncarbonated Natural Mineral Waters and Drinking Waters by Using a Modified Nested PCR-Restriction Fragment Length Polymorphism Assay. 2003;69(7):4183-4189. doi:10.1128/AEM.69.7.4183

82. Kishida N, Miyata R, Furuta A, et al. Quantitative detection of Cryptosporidium oocyst in water source based on 18S rRNA by alternately binding probe competitive reverse transcription polymerase chain reaction. *Water Res*. 2011;46(1):187-194. doi:10.1016/j.watres.2011.10.048

83. Staggs SE, Beckman EM, Keely SP, et al. The Applicability of TaqMan-Based Quantitative Real- Time PCR Assays for Detecting and Enumerating Cryptosporidium spp . Oocysts in the Environment. 2013;8(6). doi:10.1371/journal.pone.0066562

84. Giovanni GDDI, Hashemi FH, Shaw NJ, et al. Detection of Infectious Cryptosporidium parvum Oocysts in Surface and Filter Backwash Water Samples by Immunomagnetic Separation and Integrated Cell Culture-PCR. 1999;65(8):3427-3432.

85. Johnson AM, Giovanni D di, Rochelle PA. Comparison of Assays for Sensitive and Reproducible Detection of Cell Culture-Infectious Cryptosporidium parvum

and Cryptosporidium hominis in Drinking Water. *Appl Environ Microbiol*. Published online 2011:156-162. doi:10.1128/AEM.06444-11

86. Wagner-Wiening C, Kimmig P. Detection of viable Cryptosporidium parvum oocysts by PCR. *Appl Environ Microbiol*. 1995;61(12):4514-4516. doi:10.1128/aem.61.12.4514-4516.1995

87. Guy RA, Payment P, Krull UJ, Horgen PA. Real-time PCR for quantification of Giardia and Cryptosporidium in environmental water samples and sewage. *Appl Environ Microbiol*. 2003;69(9):5178-5185. doi:10.1128/AEM.69.9.5178-5185.2003

88. Kim HS, Kim D min, Neupane GP, et al. Comparison of Conventional , Nested , and Real-Time PCR Assays for Rapid and Accurate Detection of Vibrio vulnificus . 2008;46(9):2992-2998. doi:10.1128/JCM.00027-08

89. Higgins JA, Fayer R, Trout JM, et al. Real-time PCR for the detection of Cryptosporidium par Õ um. Published online 2001.

90. Verweij JJ, Schinkel J, Laeijendecker D, Rooyen MAA van, Lieshout L van, Polderman AM. Real-time PCR for the detection of Giardia lamblia. 2003;17:223-225. doi:10.1016/S0890-8508(03)00057-4

91. Majumdar N, Wessel T, Marks J. Digital PCR Modeling for Maximal Sensitivity , Dynamic Range and Measurement Precision. Published online 2015:1-17. doi:10.1371/journal.pone.0118833

92. Taylor SC, Laperriere G, Germain H. Droplet Digital PCR versus qPCR for gene expression analysis with low abundant targets : from variable nonsense to publication quality data. 2017;(February):1-8. doi:10.1038/s41598-017-02217-x

93. Yang R, Paparini A, Monis P, Ryan U. Comparison of next-generation droplet digital PCR (ddPCR) with quantitative PCR (qPCR) for enumeration of Cryptosporidium oocysts in faecal samples. *Int J Parasitol*. 2014;44(14):1105-1113. doi:10.1016/j.ijpara.2014.08.004

94. Xiao L, Singh A, Limor J, et al. Molecular Characterization of Cryptosporidium Oocysts in Samples of Raw Surface Water and Wastewater. 2001;67(3):1097-1101. doi:10.1128/AEM.67.3.1097

95. Notomi T, Okayama H, Masubuchi H, et al. Loop-mediated isothermal amplification of DNA. 2000;28(12).

96. Inomata A, Kishida N, Momoda T, et al. Development and evaluation of a reverse transcription- loop-mediated isothermal amplification assay for rapid and high-

sensitive detection of Cryptosporidium in water samples. Published online 2009:2167-2172. doi:10.2166/wst.2009.599

97. Plutzer J, Karanis P. Rapid identification of Giardia duodenalis by loop-mediated isothermal amplification (LAMP) from faecal and environmental samples and comparative findings by PCR and real-time PCR methods. Published online 2009:1527-1533. doi:10.1007/s00436-009-1391-3

98. Karanis P. Combination of ARAD microfibre filtration and LAMP methodology for simple , rapid and cost-effective detection of human pathogenic Giardia duodenalis and Cryptosporidium spp . in drinking water. 2010;50:82-88. doi:10.1111/j.1472-765X.2009.02758.x

99. Koloren Z, Sotiriadou I, Karanis P. Annals of Tropical Medicine & Parasitology Investigations and comparative detection of Cryptosporidium species by microscopy , nested PCR and LAMP in water supplies of Ordu , Middle Black Sea , Turkey. 2013;4983. doi:10.1179/2047773211Y.0000000011

100. Mahmoudi M reza, Kazemi B, Mohammadiha A, Mirzaei A, Karanis P. Detection of Cryptosporidium and Giardia (oo) cysts by IFA , PCR and LAMP in surface water from Rasht , Iran. 2013;(June):511-517. doi:10.1093/trstmh/trt042

101. Brinkman NE, Francisco R, Nichols TL, Robinson D, Iii FWS, Schaudies RP. Detection of multiple waterborne pathogens using microsequencing arrays. Published online 2012. doi:10.1111/jam.12073

102. Baeumner AJ, Humiston MC, Montagna RA, Durst RA. Detection of Viable Oocysts of Cryptosporidium parvum Following Nucleic Acid Sequence Based Amplification. 2001;73(6):1176-1180.

103. Ahmed SA, Karanis P. International Journal of Hygiene and Comparison of current methods used to detect Cryptosporidium oocysts in stools. *Int J Hyg Environ Health*. 2018;221(5):743-763. doi:10.1016/j.ijheh.2018.04.006

104. Leoni F, Gallimore CI, Green J, Mclauchlin J. Molecular Epidemiological Analysis of Cryptosporidium Isolates from Humans and Animals by Using a Heteroduplex Mobility Assay and Nucleic Acid Sequencing Based on a Small Double-Stranded RNA Element. 2003;41(3):981-992. doi:10.1128/JCM.41.3.981

105. Jellison K, Cannistraci D, Fortunato J. crossm Biofilm Sampling for Detection of Cryptosporidium Oocysts in.

106. Magar, Hend; Hassan, Rabeay; Mulchandani A. Electrochemical Impedance Spectroscopy (EIS): Principles, Construction, and Biosensing Applications. *Sensors*. 2021;21(19).

107. Houssin T, Follet J, Follet A, Dei-cas E, Senez V. Biosensors and Bioelectronics Label-free analysis of water-polluting parasite by electrochemical impedance spectroscopy. 2010;25:1122-1129. doi:10.1016/j.bios.2009.09.039

108. Pohanka M. Overview of piezoelectric biosensors, immunosensors and DNA sensors and their applications. *Materials*. 2018;11(3). doi:10.3390/ma11030448

109. Xu S, Muiharasan R. Rapid and sensitive detection of giardia Lamblia using a piezoelectric cantilever biosensor in finished and source waters. *Environ Sci Technol*. 2010;44(5):1736-1741. doi:10.1021/es9033843

110. Kramer MF, Vesey G, Look NL, Herbert BR, Simpson-Stroot JM, Lim D v. Development of a Cryptosporidium oocyst assay using an automated fiber optic-based biosensor. *J Biol Eng*. 2007;1:1-11. doi:10.1186/1754-1611-1-3

111. Wigginton KR, Vikesland PJ. Gold-coated polycarbonate membrane filter for pathogen concentration and SERS-based detection. Published online 2010:1320-1326. doi:10.1039/b919270k

112. Kang CD, Lee SW, Park TH, Sim SJ. Performance enhancement of real-time detection of protozoan parasite, Cryptosporidium oocyst by a modified surface plasmon resonance (SPR) biosensor. *Enzyme Microb Technol*. 2006;39(3):387-390. doi:10.1016/j.enzmictec.2005.11.039

113. Hinman SS, McKeating KS, Cheng Q. Surface Plasmon Resonance: Material and Interface Design for Universal Accessibility. *Anal Chem*. 2018;90(1):19-39. doi:10.1021/acs.analchem.7b04251

114. Beale DJ, Marney D, Marlow DR, et al. Metabolomic analysis of Cryptosporidium parvum oocysts in water : A proof of concept demonstration. *Environmental Pollution*. 2013;174:201-203. doi:10.1016/j.envpol.2012.12.002

115. Linden KG, Shin GA, Faubert G, Cairns W, Sobsey MD. UV disinfection of Giardia lamblia cysts in water. *Environ Sci Technol*. 2002;36(11):2519-2522. doi:10.1021/es0113403

116. Bogan JE. Disinfection Techniques for Cryptosporidium. *Journal of Dairy & Veterinary Sciences*. 2018;7(4):1-3. doi:10.19080/jdvs.2018.07.555718

117. Bradford LEA, Bharadwaj LA, Okpalauwaekwe U, Waldner CL. Drinking water quality in Indigenous communities in Canada and health outcomes: a scoping review. *Int J Circumpolar Health*. 2016;75(1):32336. doi:10.3402/ijch.v75.32336

118. Wright CJ, Sargeant JM, Edge VL, et al. Water quality and health in northern Canada: stored drinking water and acute gastrointestinal illness in Labrador Inuit. *Environmental Science and Pollution Research*. 2018;25(33):32975-32987. doi:10.1007/s11356-017-9695-9

119. Mcgregor D. *The Ethic of Responsibility*.; 2014.

120. Canada, Commission Truth and Reconciliation. SCHEDULE N: Mandate for the Truth and Reconciliation Commission. Published online 2007.

121. Statistics Canada. Ending long-term drinking water advisories. *Governmnet of Canada*. Published online 2022. https://www.sac-isc.gc.ca/eng/1506514143353/1533317130660

122. Oosterveer TM, Young TK. Primary health care accessibility challenges in remote indigenous communities in Canada's North. *Int J Circumpolar Health*. 2015;74(1):29576. doi:10.3402/ijch.v74.29576

123. Paliwal I. *DETECTION OF TRICHOMONAS VAGINALLIS, GIARDIA and CRYPTOSPORIDIUM SPP. IN REMOTE INDIGENOUS COMMUNITIES IN CANADA USING A POINT-OF-CARE DEVICE*. McMaster University; 2021.

Chapter 3: *Cryptosporidium* and *Giardia* Experimentation

Cryptosporidium and *Giardia* produce environmentally robust cysts which are infectious to human and mammal populations in both developing and developed nations. The typical method of transmission is through contaminated food or water. To limit the exposure of individuals to these pathogens, it is of interest to produce a device which can detect the cysts in water.

There are several ways that these cysts can be detected, like by microscopy, immunofluorescence, or PCR, but the traditional ways of monitoring require expensive lab equipment and chemicals, extensive technician training, and copious amounts of time spent to prepare samples. With the infectious dose of these cysts being so low, it is imperative that the time to detection be minimized, especially in remote locations, or where access to healthcare or testing facilities is low.

One such way to minimize time and the cost associated with the testing process is to fabricate a point-of-care, low-cost device with the capabilities of identifying cysts from a mixture of biological specimens. One approach to accomplish this goal is by optofluidics; a small camera connected to a Raspberry Pi will utilise shadow imaging and flow analysis of particles through a microfluidic channel to identify *Cryptosporidium* and *Giardia* cysts. The device will employ a machine learning algorithm to learn and characterize the particles in the channel when compared to other particles that may be present. This technique has been demonstrated in urinalysis for the detection of biomarker particles such as trichomonas vaginalis and red blood cells[124]. Figure 1 is a schematic representation of the device setup that has utilized shadow imaging and flow analysis for particle detection, which the proposed *Cryptosporidium* and *Giardia* device will follow utilizing a Raspberry Pi and a Raspberry Pi camera. Both surface water and drinking water are targets of testing. Surface water, found on the surface of environmental sources, will contain a higher quantity of debris, other organisms, and particulate matter that will

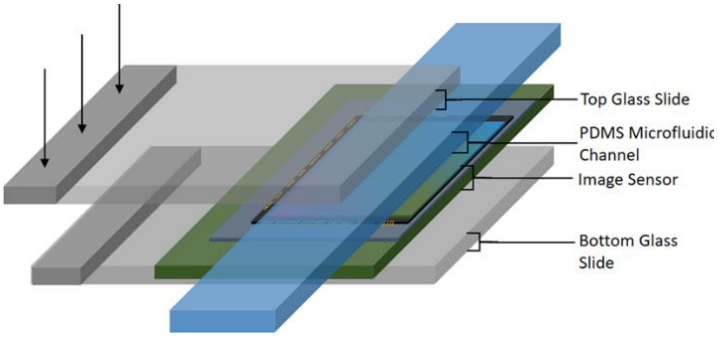

Figure 1. Schematic diagram of the setup of a microfluidic device used in shadow imaging.

need to be excluded during the detection of the (oo)cysts, potentially by pre-filtration, or by rigorous detection algorithms. Drinking water is usually pre-filtered or treated, and should contain much fewer objects which could interfere with the detection of (oo)cysts.

PDMS is employed as the material for the fabrication of microfluidic channels due to its high clarity, which reduces the interference by channel material when it comes to particle detection. Through this method, the tumbling motion of particles flowing through the channel will be analyzed by shadows created from an overhead light source. This is advantageous over traditional microscopy by giving not only morphology information but also how the particle moves during flow.

The goal of my work regarding *Cryptosporidium* and *Giardia* revolves around establishing ground truths in microscopy, and the biology and chemistry around the fabrication of the optofluidics based detection device. The ground truths are required to establish what the cysts look like so that the algorithm for tracking their movement can be developed, since the movement heavily depends on the (oo)cyst's morphology.

A non-pathogenic model was chosen to establish ground truth microscopy images; all (oo)cysts purchased were gamma irradiated and non-infectious. *Cryptosporidium parvum* was selected for these experiments, however, in future experiments, an irradiated sample of *Cryptosporidium hominis* (the more human-infective species) could be used for more specific ground truth imaging and algorithm training. *Giardia lamblia* was chosen, which is a human pathogenic model. Morphological features of the cysts chosen include the shape of the (oo)cysts which will determine the tumbling and flow pattern of the particles through a microfluidic channel.

3.1 (Oo)cyst Handling

Safety, handling, and containment procedures were followed in accordance with Pathogen Safety Data Sheets[47,48]. A sample of AccuSpike-IR, gamma irradiated, *Giardia lamblia* and *Cryptosporidium parvum* (oo)cysts, 100 each in 2.0mL of DI water, produced by Waterborne Inc, was purchased from Ceadarlane (PACIR3) and was diluted into 500mL of DI water in an amber Nalgene bottle, to protect from light degradation. An aliquot from the diluted sample was fixed onto a microscope slide with Polyvinyl alcohol mounting medium with DABCO®, antifading (SA C6164), in accordance with prior established fixing protocol[125]. Images were acquired on a Ti-U model inverted Nikon microscope with no filters.

3.2 Cryptosporidium Oocyst Morphology

As established in literature, *Cryptosporidium* cysts are circular to ellipsoidal in shape, and *Giardia* cysts are ovoid to ellipsoidal in shape. *Cryptosporidium* cysts are smaller than *Giardia* cysts; *Cryptosporidium* sizes 4.2 to 5.4µm in diameter and *Giardia* sizes 8-19µm in length[10,11,14,15,17,18,26]. Figures 2 and 3 are 40x magnification images taken of *Cryptosporidium* oocysts, taken under white light, which are small, individual oocysts that appear grouped together. Individual oocysts are circular to oval in shape, and clump in a pattern similar to water droplets on a surface.

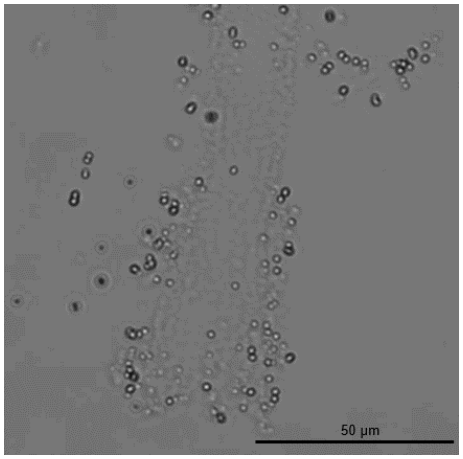

Figure 2. Cryptosporidium oocysts at 40x magnification under white light.

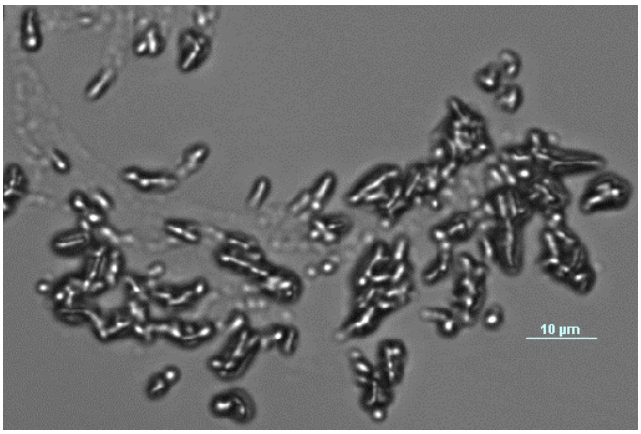

Figure 3. Cryptosporidium oocysts at 40x magnification under white light.

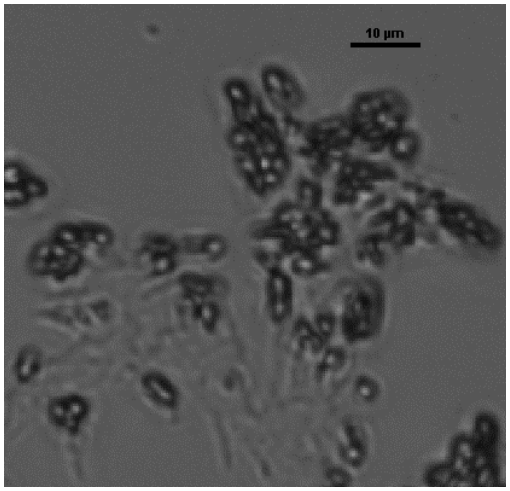

Figure 4. *Cryptosporidium* oocysts at 20x magnification under white light.

White light was used in the capture of the images since it will be used in the microfluidic platform, as well as it its simplicity coupled with how it provides information on the transparent specimen without the need for staining.

The 40x images captured were found to be the most useful at establishing morphology of the oocysts due to their size. Images were also captured at 20x magnification (Figures 4 and 5), and 10x magnification. Information provided by 10x magnification did not prove as relevant due to the size of the oocysts. 20x magnification images provided subtle differences in what was viewable by the camera; particles seem to have clearer borders and are more differentiable.

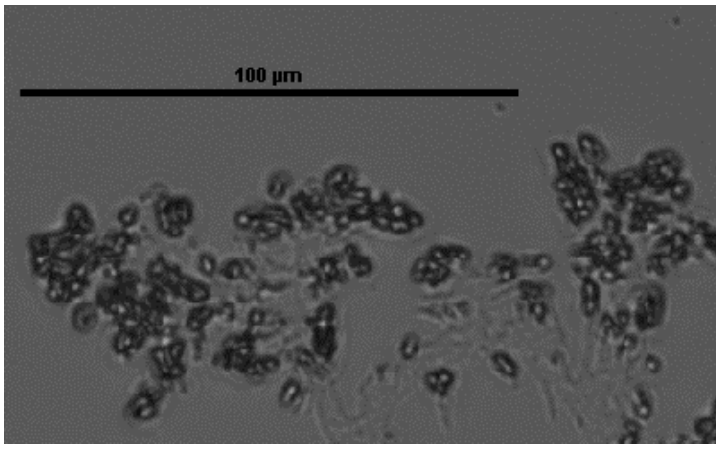

Figure 5. *Cryptosporidium* oocysts at 20x magnification under white light.

Figure 6 is a 40x magnification image taken of the oocysts under DIC, which allows for a better differentiation of individual cysts in the clumping pattern, but also shows that some of the signals in both the white light images and DIC images appear to have air bubbles contributing to the clumping pattern. DIC lighting will not be used in the microfluidic device but can provide more information in establishing a ground truth morphology to be used in creating a machine learning algorithm.

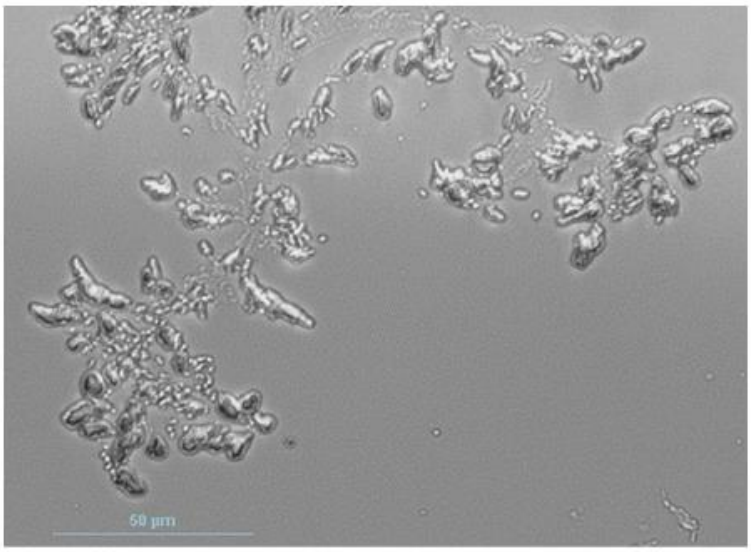

Figure 6. Cryptosporidium oocysts at 40x magnification under DIC light, showing some artifacts appear to be water bubbles.

3.3 Giardia Cyst Morphology

Figures 6 and 7 are 40x magnification images of *Giardia* cysts, identifiable by the larger size when compared to *Cryptosporidium* oocysts (Figures 2-6).

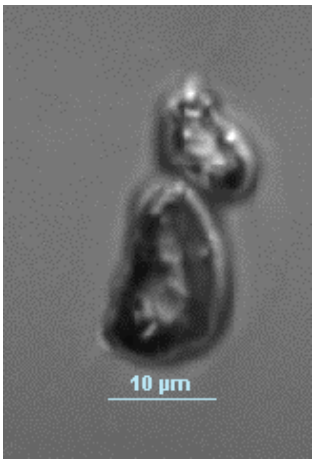

Figure 7. *Giardia* cysts at 40x magnification, under white light.

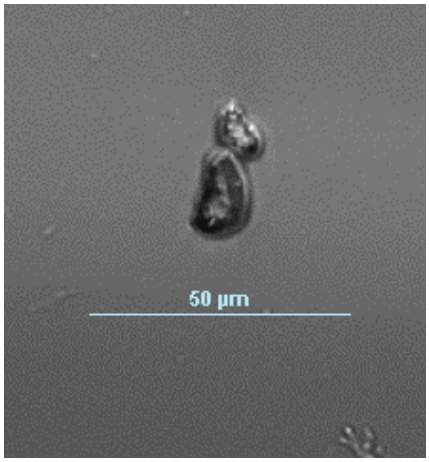

Figure 8. *Giardia* cysts at 40x magnification, under white light.

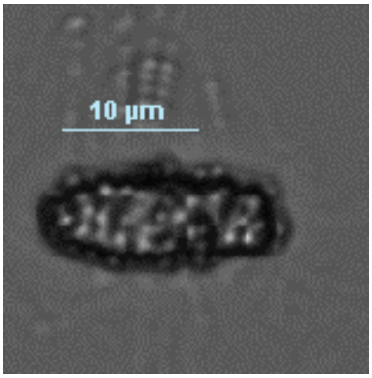

Figure 9. Predicted *Giardia* cyst at 40x magnification, under white light.

Figure 9 is a predicted Giardia cyst, based on morphology and size comparison with the other (oo)cysts in the sample. These cysts are typically ovoid to ellipsoidal in shape, but Figures 6 and 7 have a pear-shaped morphology. *Giardia* cysts can take on different morphologies. This has the potential to affect image tracking algorithms, which can be adjusted knowing that DIC imaging did not provide any further relevant information on the morphology of *Giardia* cysts

3.4 Flow of Ellipsoidal Particles

The detection of (oo)cysts flowing through a microfluidic channel will depend heavily on the tumbling motion of the particles when prompted by flow. The study of fluid dynamics of microfluidic channels has shown that there is both turbulent and laminar flow within rectangular and trapezoidal channels[126,127]. Since the (oo)cysts can be anisotropic, the size of the ellipsoid will determine the preferential direction through turbulent flow[128]. If the ellipsoid's ratio of the size of the major axis is larger than the turbulence forcing scale, the ellipsoid will travel faster in the parallel direction to its major axis, whereas if the ratio of size of the major axis is smaller than the turbulence forcing scale, the ellipsoid will travel faster in the parallel direction to its minor axis[128]. Understanding the motion of the particles which resemble the morphology of the (oo)cysts is important for the image tracking as well as in channel design.

The algorithm to identify (oo)cysts will be able to distinguish the difference in shape of the *Giardia* cysts versus *Cryptosporidium* oocysts, compared with other particles possible in a sample, and connect shape with flow mechanics to identify (oo)cysts. A video was taken of a glass microfluidic channel with 10µm polystyrene beads with the Ti-U Nikon microscope at 40x to demonstrate the flow through a channel, to be used in comparison with the Raspberry Pi and Raspberry Pi camera setup.

3.5 Microscopy Comparison

The objective lenses used to take the images on the Nikon Ti-U were 10x, 20x, or 40x, which provided a wide field of view, with the sample further away from the lens. In the microfluidic device, the camera used will have a magnification of 1, with a field of view of 1mm by 2.2mm, with a resolution of 3264 x 2448 (8-megapixel camera). The camera will be directly against the microfluidic channel, covering the entirety of the width of the channel. While the images taken on the Nikon Ti-U microscope have provide more detail about the (oo)cysts, they are relevant for determining the size and shape of (oo)cysts, used to develop the flow tracking algorithm, based on shape.

A 10x objective generally has a field of view of about 2.0mm, which is similar to the length of the field of view of the microfluidic device. Since the width of the field of view of the microfluidic device is about 1mm, increasing in magnification on the Nikon Ti-U microscope to a 20x objective would provide the field of view most like the one observed with the microfluidic device.

The morphological data gathered with the 20x will be the most similar to the data gathered with the microfluidic device, but the data gathered with the 40x objective can provide higher morphological detail for the development of the tracking organism, since it provides higher detail about the shape of the (oo)cysts. The resolution capabilities of the Nikon microscope can be up to 4096 by 4096 pixels, which is greater than the resolution provided by the Raspberry Pi camera. The video frame rate in the Raspberry Pi camera will be dependent on the use of a 5mp or 8mp camera, which are both available, with an increased number of pixels resulting in a slower frame rate of video capture due to the time taken to analyze and represent the greater number of pixels. Captured images on the Nikon were at a higher resolution and will downsample as needed during the algorithm developmental phase.

3.6 Conclusion

New optofluidic lensless imaging technology can be used to address some of the issued in POC devices, which need model biological systems for development. Most detection mechanisms for *Cryptosporidium* and *Giardia* rely on the presence of (oo)cysts, rather than live parasites, especially in environmental water samples . Non-pathogenic commercially available (oo)cysts were purchased for the development of a protocol to acquire and introduce these model systems to the Biophotonics Lab and the Mac Water microbiology lab (Dr. Schellhorn). Both model organisms are Risk Group 2 organisms and were stored in Biosafety Level 2 containment facilities in opaque containers to prevent light degradation. All microscopic images captured to identify morphological features were under transmission white light, used for comparison to what

the cysts will look like when within the microfluidic channel in the proposed device. The resulting data as guidance in the development of the microfluidic device.

3.7 Future Direction

For the next step, the (oo)cysts would need to be flown through the microfluidic channel and observed, analyzing the flow dynamics and whether the (oo)cysts will adhere to the walls of the channel. For the further development of this system, environmental waters will need to be tested. The possibility of biofilms and debris aggregating on the walls of the channel is high, and measures to combat this must be taken, such as modifying the material of the microfluidic channel. There are various ways in which the channel can be modified, but one such modification can be made to PDMS to reduce the water contact angle with the surface 15.

124. Kun J, Smieja M, Xiong B, Soleymani L, Fang Q. The Use of Motion Analysis as Particle Biomarkers in Lensless Optofluidic Projection Imaging for Point of Care Urine Analysis. *Sci Rep*. 2019;9(1):1-12. doi:10.1038/s41598-019-53477-8

125. Arrowood MJ. In vitro cultivation of Cryptosporidium species. *Clin Microbiol Rev*. 2002;15(3):390-400. doi:10.1128/CMR.15.3.390-400.2002

126. Mogus, E., Fang Q. *Modelling 3D Rectangular Microfluidic Channel Flow in a Lensless Shadow Imaging Device for Urine Analysis*. McMaster University.

127. Morini G. Laminar to Turbulent Flow in Micro-channels. *Acta Physiol Scand*. Published online 2004:2004. doi:10.1016/jbiomech.2004.06.012.

128. Yang J, Francois N, Punzmann H, Shats M, Xia H. Diffusion of ellipsoids in laboratory two-dimensional turbulent flow. *Physics of Fluids*. 2019;31(8). doi:10.1063/1.5113734

129. Gökaltun A, Kang YB (Abraham), Yarmush ML, Usta OB, Asatekin A. Simple Surface Modification of Poly(dimethylsiloxane) via Surface Segregating Smart Polymers for Biomicrofluidics. *Sci Rep*. 2019;9(1):1-14. doi:10.1038/s41598-019-43625-5

Chapter 4: Water Quality Monitoring for Ammonia

The goal of designing a point-of-care, low-cost water quality monitoring system is to create a multifunctional device capable of monitoring multiple contaminants at once. The proposed system for the *Cryptosporidium* and *Giardia* experiments, down the line, can be modified to include monitoring of other biomarkers in water, such as ammonia concentrations, which can provide information on the health of an ecosystem or the efficiency of wastewater treatment plants. Sensors monitoring dissolved oxygen, creatine, and pH have been successfully designed and produced as microfluidic devices, as well as the use of motion analysis for point of care urine analysis[124,130,131].

The *Cryptosporidium* and *Giardia* channel utilizes shadow flow imaging through a microfluidic channel and an overhead white light source to identify biomarkers flowing through a fluid, similar to Figure 1. With this setup, it is possible to modify the materials which the channel is made of to add the functionality of detecting another biomarker. A hydrogel with a stability similar to the PDMS channel in Figure 1 with ammonia sensing capabilities would improve the use of a microfluidic water quality monitor. Experiments were completed to identify the possibility of fabricating such a hydrogel for ammonia detection, and to see its feasibility in combining the platform with the shadow imaging flow analysis of *Cryptosporidium* and *Giardia* (oo)cysts.

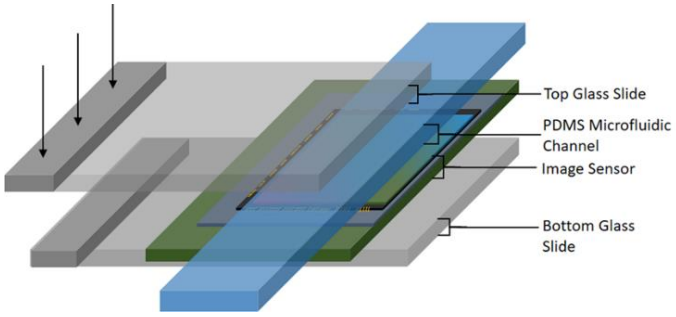

Figure 1. Schematic diagram of the setup of a microfluidic device used in shadow imaging.

4.1 Ammonia as a Contaminant

Ammonia is an important nutrient in aquatic environments due to its role in the aquatic nitrogen cycle as well as its impact on organism growth. The analyte can be accumulated in waterways and marine and estuarian environments by various methods, though it is typically unusual to find it in large quantities. The effect and toxicity of the compound on organisms is dependent upon the chemical form of ammonia, the pH of the water, and the temperature[6]. Below the pH of 8.75, ammonium (NH_4^+) is the predominant

form, which is generally non-toxic, whereas above pH of 9.75, the dominant form is toxic ammonia (NH_3)[132].The pH of an aquatic environment is dependent on other factors. While the relatively non-toxic form is generally the most abundant form, excessive concentrations can still be dangerous to aquatic life. Excess quantities of the toxic form of this compound, such as 0.5μmol, will physiologically alter the gills, kidneys, livers, and other organ tissues of aquatic organisms, which can ultimately lead to death[6,133]. In an organism, it can cause cell damage and affect the levels of oxidative stress, which can alter fish behaviour by reducing swimming activity and foraging behaviour in fish[6]. Both ammonia and ammonium can stimulate the production of phytoplankton which can lead to rapid algal growth; ammonia and ammonium can be converted into nitrate by nitrifying bacteria[132]. Eutrophication is a result of increased concentrations of nutrients in surface water, with nitrate, nitrite, and ammonia being contributing factors[7].

The increases in nutrients can have many negative impacts on an ecosystem, some which can affect humans. With excess amounts of nitrogen, fish populations can drop due to direct death or alteration of food sources. Over production of algae, especially on the surface of a waterway, can change the light distribution to species living below the surface. With temperature changes due to light distribution, species may die off or reconfigure to survive, which could result in pH, dissolved oxygen, salinity, or other nutrient changes. The catastrophic effects may be entire ecosystem death, or in a less severe case it may render a water source unsuitable for human use.

4.2 Sources of Ammonia

There are a multitude of ways in which water quality can be impacted, both by human and natural influences. Geological, climatic, and hydrological emissions are of the most influential natural mechanisms by which water quality is affected[7]. If water levels fall, the concentration of salts in the remaining water may rise, which can directly affect organisms or alter the availability of nutrients which affects organisms in a longer term. The analyte can also amass as a by-product of protein metabolism from fish and invertebrates, from phytoplankton and organic matter decomposition, and can be utilized by nitrifying bacteria to form nitrate [4,132]. Nitrogen mineralization, organic sediment nitrogen, and coliform bacteria are other contributing factors[134,135].

Some of the most frequent anthropogenic methods of accumulation are agricultural runoff, landfill contamination, wastewater pollution, and industrial emissions. In a study of 248 hotspots which had local ammonia enhancement, the 83 agricultural spots were consistently determined to be associated with animal farming[136]. In the same study, the 158-spot class of industrial related hotspots, the majority (over 130) were found to be associated with ammonia-based fertilizer manufacturing. Other works have shown that

leaky sewers, leaky mains, on site sewage disposal, septic tanks, landfills, gasworks, atmospheric deposition (which is polluted by human interaction), highways and roads, airfield de-icing, and house building were other sources of groundwater nitrogen[137]. Particularly, contaminants from municipal solid wastes landfills are more diverse than from industrial or agricultural sites[138].

Diverse forms of contaminants pose a challenge to many commercially available aqueous ammonia detection methods, which rely on pH changes to dictate ammonia concentrations. Contaminants may be upstream in an ammonia production pathway, which can make it difficult to rely on pH indicators for ammonia concentration determination. The pH, however, does affect the proportion in which the two forms of nitrogen (ammonia and ammonium) present themselves. Not only does a challenge arise when regarding pH, but the high salinity of saltwater environments can affect the analysis of the analyte when it is found at trace concentrations at the nanomolar level[132].

4.3 Ammonia Detection Methods

Ammonia detection has been completed via multiple routes. It can be detected in ways such as optically, electrochemically, and biologically. Each method of detection has strengths and weaknesses, and some are more developed than others.

4.3.1 Optical Detection

The first approach for the detection of ammonia is through analyzing the optical properties of various substances, which is typically done through spectrophotometric methods, fibre-optic detection, or fluorescence emission detection, though other optical methods do exist[133]. The IPB (indophenol blue) methods, which is based on the Berthelot reaction, produces indophenol blue when ammonia nitrogen reacts with hypochlorite and phenol, producing a colour change with a maximum absorbance at 640nm[133,139]. This reaction utilises phenol, which is corrosive and toxic, but is commonly replaced with salicylic acid, thymol, or OPP (o-phenylphenol)[133]. This method of detection is being optimized for flow analysis, including solid phase extraction, flow injection, and microfluidics to achieve automatic processing with limited sample processing[133].

Fluorescence detection is another optical based method which is used in ammonia nitrogen detection. For example, o-phthalaldehyde (OPA) and sodium sulfite reacted in an alkaline medium form an ammonia reactive fluorescent compound[133,139]. Quantum dots (QD) are an attractive alternative to traditional organic dyes, due to strong photobleaching resistance, wide absorption spectra, and narrow emission spectra.

Coupling fluorescence detection with flow analysis, microfluidics, micro-electromechanical systems, and/or solid phase extraction can achieve a higher sensitivity and optimized limit of detection (LOD) of 1.2nM[133].

The most common form of optical detection of ammonia relies on colourimetric pH detection. These methods rely on indirect measurements of ammonia via pH changes. Chemicals imbedded into paper test strips can be dipped in water, with a pH indicator (typically Bromothymol blue) reading the transformation of ammonium into ammonia[133]. This method can also be employed in ammonia gas detection. These methods usually have wider ranges of pH that a test can fall within and are semi-quantitative.

Fibre optic detection is a newer method in development for the use of ammonia detection. Methods utilizing fibre optic technology rely in changes in refractive index of fibre material coating, which causes a wavelength or power level shift in the transmission response when ammonia reacts with the coating material[133]. Utilizing loss mode resonance, a porphyrin combined with titanium dioxide was used to detect aqueous ammonia with a LOD of ~5.88μM[133].

Optical methods of detection have the potential benefit of being simple and can be made to be low cost with inexpensive chemicals and equipment. Miniaturization is another possible benefit, with the implementation of microfluidic devices. These methods generally require chemicals, which may leech into the environment when deployed in field, but can be made to be environmentally inert.

4.3.2 Electrochemical Detection

Ammonia nitrogen can be detected by analyzing electrochemical properties of a solution. Electrochemistry is one convenient method which provides rapid results. Gas sensing electrodes utilize a hydrophilic permeable membrane which separates ammonia and encapsulates an internal solution of ammonium chloride[133]. With a pH adjustment to highly basic (>11), ammonium chloride is converted to ammonia and travels to the internal solution through the gas-sensitive membrane[133].

Ion-selective electrodes utilize a sensitive membrane, and when the probe is placed in a water sample, a potential is created between the inside and outside of the membrane[133]. These electrodes have a high and unique ion-selectivity, with short response times and high sensitivity.

Electrodes that are modified with nanomaterials can have high sensitivity and selectivity and provide rapid analyte detection[133]. Using voltammetry, oxidation/reduction

current is measured under the electrode potential. One example of a nanomaterial modified electrode in the detection of ammonia is carbon nanotubes[133].

4.3.3 Biological Detection

Biosensors use a biochemical receptor that is in direct contact with a transducer, and when the analyte of interest is recognized, a reaction occurs which is converted to a quantifiable electrical signal by the chemical or physical transducer[133]. The use of biological processes in the detection of ammonia is a relatively new process, and data can be gathered by the measurement of current or voltage.

4.4 Ammonia Sensor Development

The goal of this device is to provide a low-cost, point-of-care device for water quality monitoring. In remote and Indigenous communities, costs and the time associated with water testing can be high when technicians need to be transported to collect samples and samples need to be returned to an external lab for testing. Having a device that can be deployed in field without the need for an expertly trained technician, with data that can be wirelessly uploaded to a site with open access, would make routine monitoring data more accessible. Continuous water quality measurements would be beneficial for long term studies regarding aquatic environments and life, for example, the prediction of algal blooms.

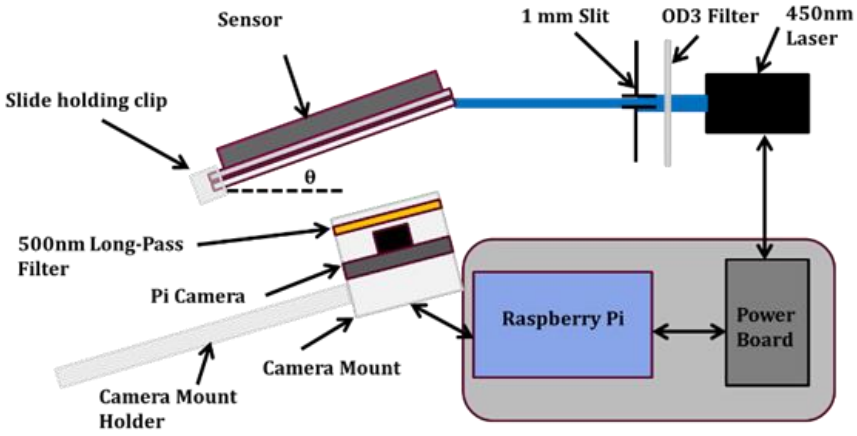

Figure 2. Schematic of setup for the laser based, TIRF mechanism for the detection of gaseous ammonia.

4.4.1 Sensing System Design

The detection of ammonia through fluorescence was previously worked on by a former Ph.D. student, Eric Mahoney, who worked towards using a thin film cellulose acetate Eosin coating on a microscope slide, excited by a TIRF laser source, with a PDMS microfluidic channel cap. The device utilized a Raspberry Pi camera to detect the intensity of a fluorescence response upon the diffusion of ammonia gas through a gas permeable membrane to contact the immobilized Eosin dye. This method requires the use of an aligned laser, which makes the system very sensitive to offsetting movements, requires extensive protection to contain the beam, personal protective equipment, and a strong power source. A self-contained housing unit was prototyped, but the entire system needed further optimization to be fully functionalized. An alternative approach was taken, utilizing a fluorescence responsive, aqueous ammonia detecting hydrogel, with lower costs, fewer safety concerns, and fewer high precision steps.

4.4.2 Introduction to Hydrogels

A hydrogel is a crosslinked polymerized material that is not water soluble, which are used heavily in the field of biomedical engineering. According to solvents, the gels are fabricated as three-dimensional network chemically or physically crosslinked by entangled molecular bonds and interactions[140]. Many hydrogels are soft and flexible in nature, with high human biocompatibility, and insolubility in water once fabricated, making them an attractive method for biomedical applications such as drug delivery and wound dressing[141]. They are capable of being stimulus-responsive, in some cases providing a luminescence response upon interaction with a target molecule[140]. Hydrogels have been imbedded with Lanthanide ions, organic dyes, luminescent small molecules, semiconductor particles, and carbon to provide an array of stimulus responsive gels[140,142–146].

4.4.3 Fabrication of a Europium, Polyvinyl Alcohol, Formamide Hydrogel

To improve upon Eric's ammonia sensing design, an alternative approach was explored using a formamide hydrogel matrix containing Europium (Eu^{3+}) molecules, which has been shown to demonstrated in ammonia detection[147–149]. Other previous works have demonstrated the use of Eu^{3+}or other solutes to provide a luminescent response upon interaction with a stimulus, many of which are used as ammonia detectors[140,142–147,150–153]. The fabrication costs of this hydrogel were calculated to be ~$20CAD for 15mL, using products purchased from Sigma Aldrich (SA): Europium chloride hexahydrate (SA 212881), Salicylic acid (SA 247588), Poly(vinyl alcohol) (SA 341584), Formamide (SA F9037), Sodium Hydroxide (SA 221465), 2-Thenoyltrifluoroacetone (SA T27006), and ThermoFisher Scientific (TF): Formamide (TF 014835.30). All chemicals were used as received. The hydrogel approach was explored for its low-cost fabrication method, chemical inertness to aquatic life, and fluorescence recovery capability[148,149,154,155]. The implementation of a UV-LED (Thorlabs LED385L) with wavelength 385nm, and a UV filter (Thorlabs FEL0500) offer a lower cost alternative to the laser implemented in Eric's work.

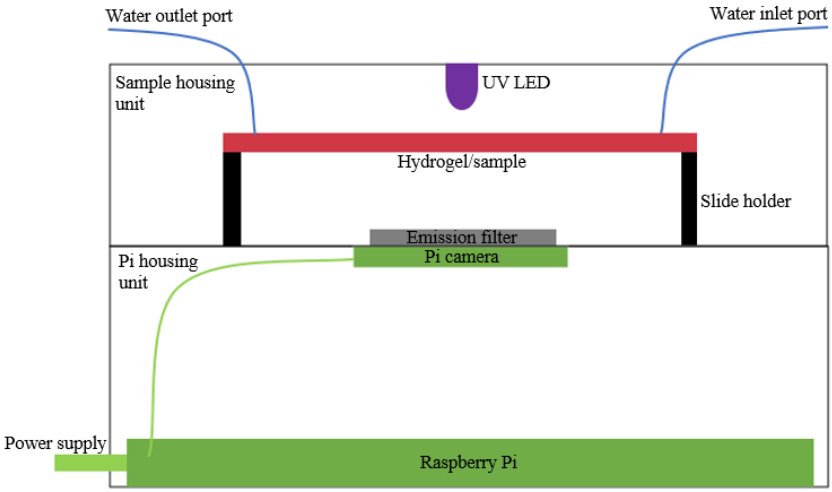

Figure 3. Schematic illustration of proposed ammonia detection unit.

The proposed gel would have recoverable fluorescence quenching ability that can be temporally measured, with the hypothesis that the time for fluorescence quenching to occur would be directly correlated with the concentration of ammonia in a sample. This could be measured by pixel intensity, monitored with a Raspberry Pi camera in a dark environment, with a UV filter placed over the camera to filter out potentially interfering excitation light. The proposed diagram is shown in Figure 1 and would contain two

separate chambers within a water-resistant box, one housing the sample while the other contains the electronic components. The separation of the sample from the electronics would limit the possibility of damage occurring to the electronic components should the inlet and outlet ports for the aqueous sample happen to leak. A filter holder was designed and printed from PLA filament, with a slot for the Raspberry Pi camera to slide in directly underneath. The whole proposed containment unit would be less than 30cm by 30cm, making the device small and portable.

Based on other works, a hydrogel fabrication protocol was followed[147,148]:

1. Add to 15mL Fm and stir vigorously at 90^{O}C for 1h
2. 0.5mmol Eu(Cl)3•6H2O
3. 1mmol Sal
4. 1mmol NaOH
5. Add 0.15g TTA and stir at 90oC for 1h
6. Add 1.5g PVA and stir vigorously at 95^{O}C for 5h
7. Immediately put in -20^{O}C fridge for 12h
8. Freeze dry for 10h

Table 1. Physical observations of chemical ingredients

Chemical	**Physical Observation**
Europium Chloride Hexahydrate ($EuCl•6H_2O$)	Small, white crystals
Salicylic acid (Sal)	Fine, white powder, crystalline
Poly(vinyl alcohol) (PVA)	Fine, white powder, sand like
Formamide (Fm)	Clear, colourless liquid
Sodium hydroxide (NaOH)	White, hemispherical solid pellets
2-Thenoylfluoroacetone (TTA)	Clear, colourless liquid
Dimethyl Sulfoxide (DMSO)	Clear, colourless liquid

Since the prior established protocol did not give direct quantities of chemicals, the required quantities were calculated as follows:

$Eu(Cl)_3 \bullet 6H_2O = 366.41 g/mol$	$Sal = 138.12 g/mol$	$NaOH = 40.00 g/mol$
$n = \frac{m}{MW}$	$n = \frac{m}{MW}$	$n = \frac{m}{MW}$
$0.0005\ mol = \frac{m}{366.41}$	$0.001\ mol = \frac{m}{138.12}$	$0.001\ mol = \frac{m}{40.00}$
$m = 0.0005\ mol \bullet 366.41$	$m = 0.001\ mol \bullet 138.12$	$m = 0.001 mol \bullet 40.00$
$m = 0.1832 g$	$m = 0.1381 g$	$m = 0.04 g$

The experiment was completed in a fume hood. A hot plate was plugged in and set to 90^{O}C. A 100mL glass beaker was placed on top of the hot plate and a magnetic stir bar was added. 15mL of Formamide was measured in a graduated cylinder and added to the beaker, and the magnetic stir bar was turned on. 0.18g of EuCl•6H_2O was measured on a tared digital balance in a weigh boat and set aside. 0.14g of Sal was weighed on the balance and set aside. 0.04g of NaOH was weighed on the balance and set aside. The three measured chemicals were added to the Fm in rapid succession. Upon adding the

Figure 4. Hydrogel solution upon adding EuCl•6H_2O, Sal, and NaOH to Fm.

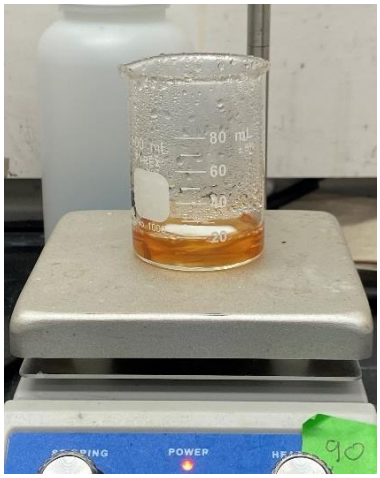

Figure 5. Hydrogel solution upon the addition of PVA, burnt orange colour.

chemicals, the solution turned a light, translucent yellow colour, and had the viscosity similar to water (Figure 4).

After 1h of stirring at 90^{O}C, 0.15g of TTA was measured on the balance and added to the solution and let to mix for 1h. Within 30m of mixing, the solution turned burnt orange in colour (Figure 5) but was kept on the hot plate mixing for another 30m. After 1h of mixing, 1.5g of PVA was measured on the balance and added to the solution.

Figure 6. Hydrogel mixture after the addition of PVA, thick brown gelled substance.

Upon addition of the PVA, an immediate puff of white vapour was observed, and the solution began to coagulate, turning brown, and emitted a strong burnt odour. The heat was turned off and the beaker was removed from the plate. The coagulated solution was poured into a small petri dish and left to cool (Figure 6). The first attempt at hydrogel fabrication was deemed unsuccessful, which is expected to have been due to solvent evaporation.

Using a different hotplate, with a digital temperature display the above protocol was repeated, with a glass dish placed overtop of the beaker to prevent evaporation of the solvent (Figure 7) the previously listed protocol was attempted again.

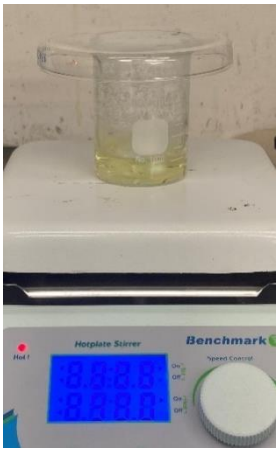

Figure 7. A glass dish on top of the hydrogel to prevent solvent evaporation.

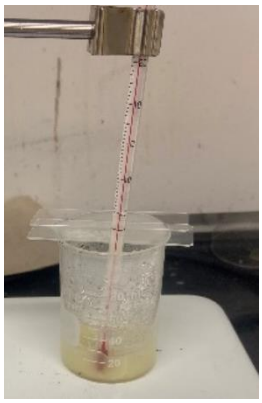

Figure 8. An analog thermometer held in the reaction solution, with glass microscope slides to prevent solvent evaporation.

Figure 9. Microscope slide after taking it out of the -20^{O}C freezer, with particulates and inconsistent freezing.

Upon addition of PVA, particulates were observed swirling in the solution. At the 5h mark of mixing, the particulates of PVA were still observed. An analog thermometer was obtained, and the solution temperature was measured to be <70^{O}C. A stand was obtained to hold the thermometer in the solution, and a glass microscope slide was used to cover the beaker (Figure 8). The temperature was set to 135.0^{O}C on the digital thermometer and a temperature of 95^{O}C was observed on the analog thermometer, and the solution was left to stir for 5h. After 5h of stirring, smaller particulates of PVA were observed in the solution, and the viscosity appeared to have increased. The solution was poured into a small petri dish and onto a glass microscope slide (which was placed into a 50mL Falcon tube for stability) and was placed into a -20^{O}C freezer for 12h. After 12h, the petri dish and microscope slide were removed from the -20^{O}C freezer (Figure 9) and placed into a freeze dryer at the Biointerfaces Institute. Before freeze drying, the solution was observed to be non-homogenous, containing particulates and inconsistent freezing (Figure 9). This

result is expected to be caused by insufficient time or temperature of the sample, leading to the PVA not dissolving properly. After a discussion with a technician at the Biointerfaces Institute, it was determined that any volumes of sample larger than the small petri dish and microscope slide would have the potential to damage the freeze dryer as it was designed to dry samples with water used as solvent.

Regardless, the freeze drying was unsuccessful, the samples were still liquid upon removal from the freeze dryer. The protocol was attempted again, with the analog thermometer and microscope slide present from the beginning (Figure 10).

At 4h into the final stirring step, large PVA particulates were still observed, so the solution was removed from heat and poured into two (2) separate 10mL conical tubes. In one tube, 1.88mL of deionized (DI) water was added to 7.5mL of reaction solution to make an 80% Fm in water solution. The rest of reaction solution was poured into a different tube. Both tubes were sonicated for 2 minutes. Cloud like formations appeared while sonicating but were redispersed with tube agitation. After 2 minutes, the tubes solutions were poured into two (2) separate beakers and were returned to heat and stirring for 1h. The particulates in both solutions were observed as much smaller and finer. After 1h of stirring on the hotplate, both solutions were poured into small, labelled petri dishes and placed in a -20^{O}C freezer. The viscosity of both solutions was higher than the previous experiment, with the solution containing no DI water having a higher, syrup-like viscosity, while the solution containing water was like sugar-water. The solution remaining in both beakers after pouring immediately began to gelatinize.

Figure 10. Addition of an analog thermometer to the experiment chamber to measure temperature more accurately.

The addition of DI water was completed to see if changing the solvent composition would improve the solubility of PVA, as most protocols utilize DI water or DI water/organic solvent mixture as a solvent[141,154,156–165].

4.4.4 Freeze Thaw Method and PVA Polymerization

After 15h of freezing at -20^{O}C, a cyclic freeze-thaw protocol was adopted (Table 2), in lieu of a freeze dryer. The protocol was designed after a paper published in 2000 outlining the structure and morphology of freeze/thawed PVA hydrogels[166], with consideration from multiple other works[161,164,167–171]. Freeze-thaw methods are comparable to freeze-drying since they produce a similar structural result. The concept of a freeze that method is based on the formation of solid solvent crystals at low temperature, which will displace solutes when freezing occurs. Pushing the PVA particulates together into a close spatial relationship allows for the coordination and formation oh hydrogen bonds, which is the solidification process in physically linked PVA hydrogels[141,157,161,162,164,165,170,172]. Figure 11 is a representation of the freeze-thaw process to coordinate hydrogen bonding, with the end diagram representing when the solvent has been removed, whether by evaporation or by freeze-drying. PVA hydrogels can also be chemically cross linked, but that would require additional chemicals which could damage the ammonia-responsivity of the attempted hydrogel[141,156,157,160–163,170].

Table 2. Freeze-thaw cycles of PVA hydrogel.

State	Time (h)	Temp (^{O}C)	Start	Finish
Frozen	15	-20	Wed 7:30pm	Thurs 10:30am
Thaw	4	22	Thurs 10:30am	Thurs 2:30pm
Frozen	5	-20	Thurs 2:30pm	Thurs 7:30pm
Thaw	4	22	Thurs 7:30pm	Thurs 11:30pm
Frozen	8	-20	Thurs 11:30pm	Fri 7:30am
Thaw	4	22	Fri 7:30am	Fri 11:30am
Frozen	8	-20	Fri 11:30am	Fri 7:30pm
Thaw	4	22	Fri 7:30pm	Fri 11:30pm
Frozen	8	-20	Fri 11:30pm	Sat 7:30am
Thaw	4	22	Sat 7:30am	Sat 11:30am
Frozen	8	-20	Sat 11:30am	Sat 7:30pm
Thaw	4	22	Sat 7:30pm	Sat 11:30pm
Frozen	8	-20	Sat 11:30pm	Sun 7:30am
Thaw	4	22	Sun 7:30am	Sun 11:30am

A total of 7 freeze-thaw cycles were completed at -20^{O}C and 23^{O}C (room temperature). An increased number of freeze-thaw cycles can increase crosslinking, which is why 7 cycles were completed as opposed to 3 to 5[166]. Figure 12 shows the hydrogels after removing from the -20^{O}C freezer following the 15h freezing step. On the second cycle, when removing the samples from the freeze component, a physical change was observed in the sample with no DI water. The sample transformed from a clear gel to a white opaque gel (Figure 13), starting at one outside edge of the dish and migrating across the sample. The sample with DI water remained unlinked after the seventh cycle of freeze-thawing (Figure 13). In an attempt to link the gel, the sample was placed in an oven at 37^{O}C for 5h[149]. The gel was ruined by another student in the shared lab space who did not check the oven before turning up the temperature to 70^{O}C, despite a note that was left on the door indicating when the sample would be finished processing (the student claimed to have not seen the note). The gel deformed and dried out completely, while the petri dish melted and deformed. The successful gel was stored in the -20^{O}C freezer when not in use.

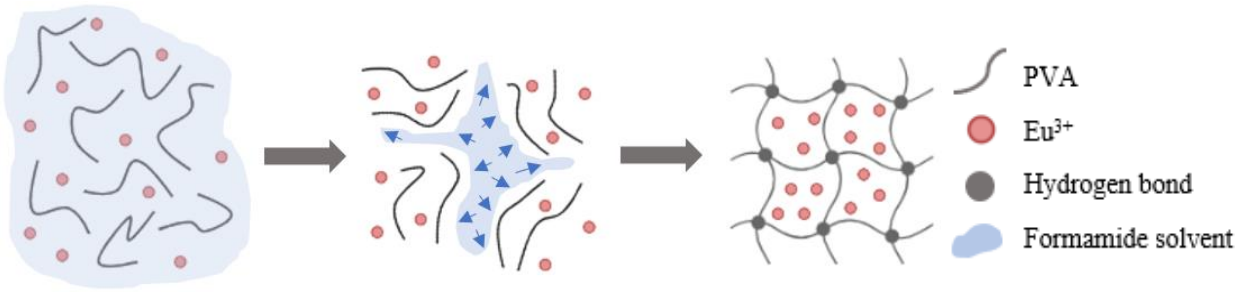

Figure 11. Schematic representation of the freeze-thaw process, coordinating hydrogen bonds to form a solid.

Figure 12. Hydrogels removed from the -20^{O}C freezer after freezing for 15h.

Figure 13. Hydrogels following 7 cycles of freeze-thawing, with H_2O was still liquid while no H_2O was solid.

4.4.5 Excitation and Emission of Ammonia Sensitive Hydrogel

The excitation and emission data about the gel has been established in literature[148,149]. Figure 14 (Wang 2019) shows there is an excitation maximum around 365nm, and an emission spectrum at 619nm. The commercially available UV-LED purchased from ThorLabs uses 385nm light, which falls just outside the peak, and provides adequate excitation for the gel.

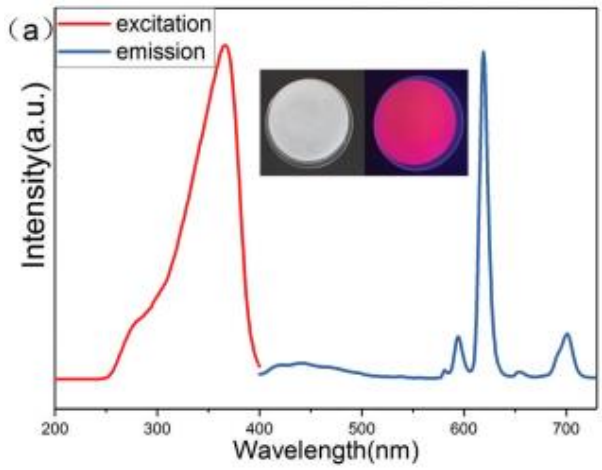

Figure 14. Pre-established excitation and emission data of the Fm/PVA/Eu hydrogel (Wang 2019).

The successfully solidified gel was tested for ammonia response. Prior to testing for ammonia response, the gel was illuminated with the 385nm UV-LED to establish a baseline intensity (Figure 15). A tap water sample was deposited onto the surface of the gel to determine whether any response would be observable from a solution containing no aqueous ammonia. There was no observed response from the gel upon tap water contact. A preprepared 5ppm ammonia solution was then deposited onto the gel and the response was observed. Upon initial contact, the intensity of the gel increased (Figure 16). Following ~30s of incubation, the intensity of the gel dropped overall, and was slowly quenched from initial contact site outwards, as the ammonia solution migrated across the gel (Figure 17).

The solution was then removed from the gel and fluorescence was observed (Figure 18). The fluorescence intensity of the gel decreased dramatically following the incubation with the ammonia solution, proving the gel successfully produced an ammonia response.

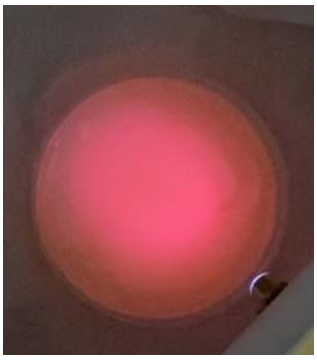

Figure 15. Hydrogel with no sample under 385nm light.

Figure 16. Hydrogel upon initial contact with 5ppm ammonia solution under 385nm light.

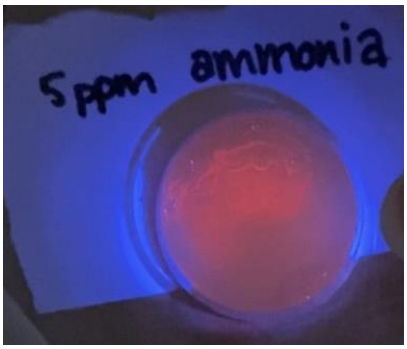

Figure 17. Fluorescence quenching caused by 5ppm ammonia under 385nm light.

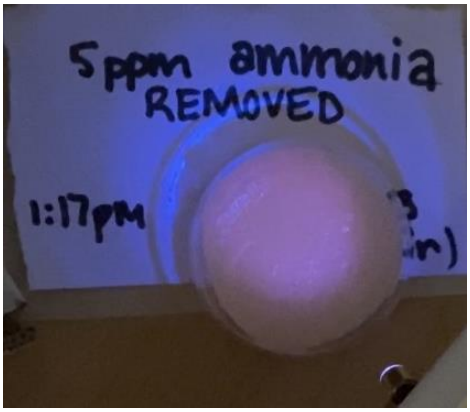

Figure 18. 5ppm ammonia solution removed from the hydrogel, under 385nm light.

The gel was placed back in the -20^{O}C freezer. The following day (~24h of elapsed time), the gel was removed from the freezer to observe fluorescence recovery. There was a very minute fluorescence recovery observed, indicating the need for improvement of recovery mechanism (Figure 19). The gel was placed back into the -20^{O}C freezer. 2 months later, the gel was removed and tested for fluorescence recovery once again (Figure 20). An increase in fluorescence, when compared to the observation recorded after 24h of recovery time, was observed, though not to the original intensity, indicating a further need for improvement of fluorescence recovery.

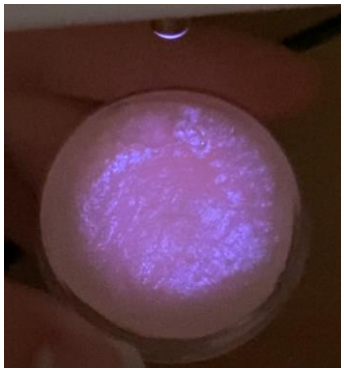

Figure 19. Fluorescence recovery of the hydrogel after 24h, under 385nm light.

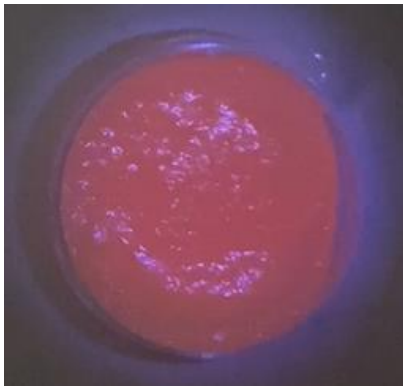

Figure 20. Fluorescence recovery of the hydrogel after 2 months, under 385nm light.

The successful fabrication of the hydrogel indicated the need for a mechanism of depositing the gel onto a microscope slide, like proposed in Figure 3 and Figure 21. A 3D model of a hydrogel holder was designed in AutoCAD and 3D printed with PLA filament on a Creality CR-6 SE 3D printer. The holder was then attached to a microscope slide

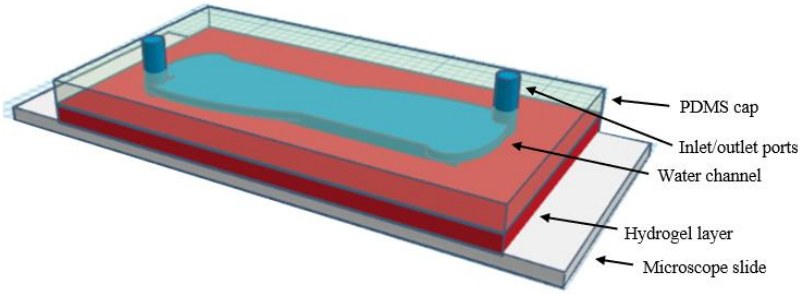

Figure 21. Schematic representation of proposed setup of a microfluidic channel incorporating ammonia sensitive

Figure 22. Microscope slide with binder clips, mold for hydrogel casting.

with miniature binder clips (Figure 22). This design would allow for the hydrogel to be directly poured onto the slide from the beaker, and conveniently had carrying handles based on the design.

Despite following the identical procedure as in the experiment which successfully produced a solid gel, subsequent attempts are gel fabrication were unsuccessful (Figure 23), and remained liquid after freeze-thaw cycling. It is unknown why the subsequent attempts were unsuccessful, but could be due to PVA not dissolving at a high enough degree. The unsuccessful attempts at fabricating the gel were left out at room temperature, and evaporation of solvent was observed. A red colour was also observed in the samples (Figure 24). The proposed reason for the red colour is due to the interaction of the gel with the 3D printed PLA material, as the red was not observed in the sample poured into a small petri dish.

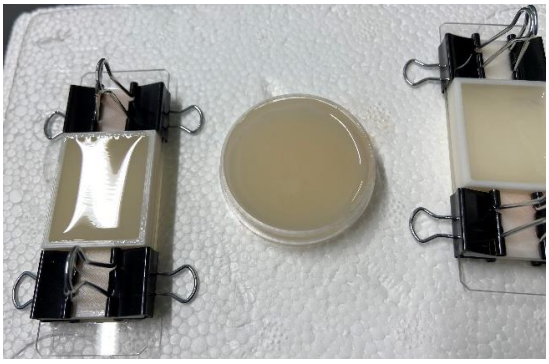

Figure 23. Unsuccessful subsequent attempts at hydrogel fabrication.

Figure 24. Solvent evaporation and red colour observed.

\

4.4.6 Solvent Modifications for Increased Mechanical Stability

Modifications to solvent were explored in an attempt to increase the possibility for solidification and mechanical stability of the gel. Consultation with McMaster professor Dr. Todd Hoare in the Department of Chemical Engineering led to the suggestion of implementing Dimethyl Sulfoxide (SA D8418). The theory behind using DMSO comes from the lack of a amine group in the compound, which could have caused some steric hinderance in the gels using Fm (Figure 25). DMSO has two methyl groups attached to the central sulfur molecule (Figure 26), which increases the number of hydrogen atoms available to make hydrogen bonds.

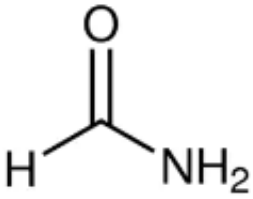

Figure 25. Schematic representation Formamide.

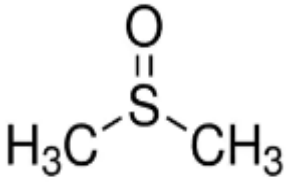

Figure 26. Schematic representation of DMSO.

The above protocol was completed with DMSO in place of Fm. The solution took on a more slippery look, with a slight green tint (Figure 27). Upon the addition of PVA, the viscosity increased immediately, and it took on a melted gel quality. When removed from the hot plate after 5h of stirring, the gel was poured into a medium petri dish and an adapted microscope slide and placed into the -20^{O}C freezer to begin a freeze-thaw cycle of 7h and 3h respectively. The gel solidified from the outside inwards (Figure 28). The gel poured into the adapted microscope slide solidified in a non-uniform manner (Figure 29).

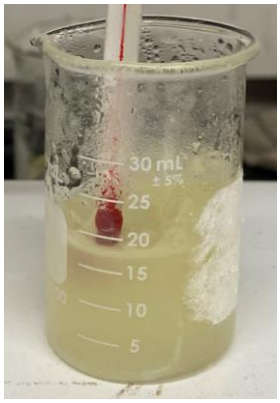

Figure 27. Hydrogel fabrication with DMSO.

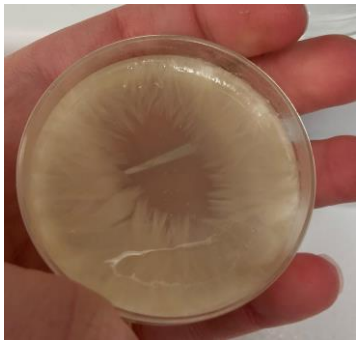

Figure 28. Freezing of DMSO hydrogel after first step of freeze-thaw.

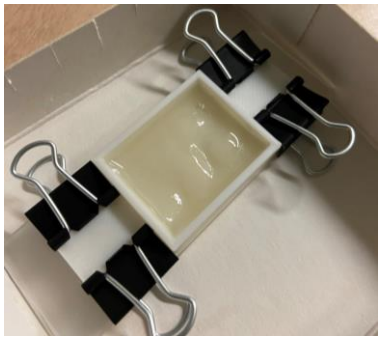

Figure 29. Hydrogel poured into microscope slide adapter, solidified non-uniformly.

When the freeze-thaw cycling was complete, it was observed that the gel did not stick to the adapted microscope slide, it had come up from the edges, and a clear, colourless liquid was pooling around and on top of the gel. The liquid was removed with a micropipette and put into a microcentrifuge tube. The samples and the removed colourless liquid were viewed under the UV-LED, which all fluoresced (Figures 30, 31, and 32). The liquid fluorescing indicated that Eu^{3+} was leeched out of the gel and into the liquid. The petri dish sample was then tested for ammonia response; tap water and 5ppm ammonia solution were both deposited onto the gel and exhibited the same lack of increase or quenching of fluorescence (Figure 33).

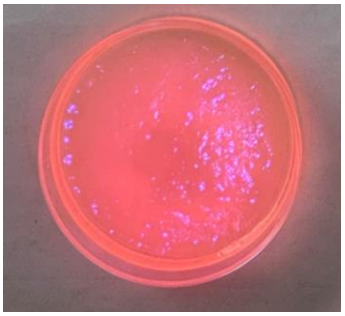

Figure 30. DMSO hydrogel under 385nm light.

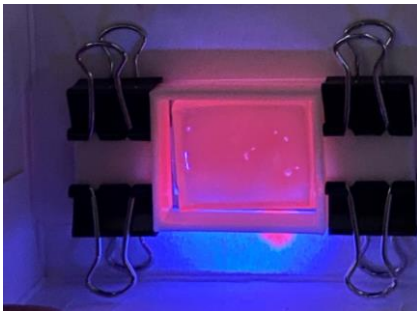

Figure 31. DMSO hydrogel in microscope adapter, under 385nm light.

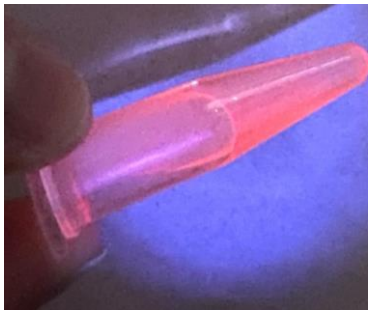

Figure 32. Removed liquid from microscope adapter sample, under 385nm light.

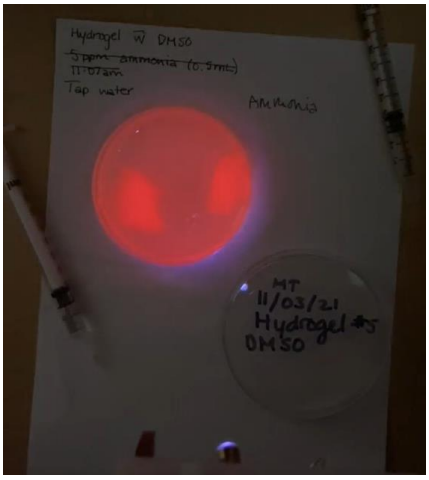

Figure 33. Tap water and 5ppm ammonia solution on DMSO hydrogel, no ammonia response.

Further experiments with mixed solvents were completed. Mixed solutions of water and Fm, and Fm and DMSO were used as solvents in fabrication of the hydrogel. Both experiments produced a solidified gel, but neither experiment's product produced an

ammonia response. The conclusion that can be drawn from this is that the Fm is a vital component of the ammonia response mechanism. A search into the functions of all of the chemicals in the experiment was done.

The TTA is used as an organic sensitizer, and provides oxygen donor sites, leading to a thermodynamically stable Eu^{3+} complex[173]. The complex formed promotes the transfer of energy so that Eu^{3+}, and the TTA acts as an antenna, enhancing luminescence[173,174]. TTA acts as a chelating organic ligand, which can form with lanthanide ions such as Eu^{3+} into a complex, where it becomes a photosensitizer by absorbing light and tightly chelating it[174]. Sal, an aromatic carboxylic type ligand, is also used as a coordinating agent, working to sensitize Eu^{3+} though forming a stable complex and utilizing the antenna effect[175–177]. Sal also absorbs UV light and transitions electrons with the aromatic carboxylic acid group, and the transfer of intramolecular energy[175].

Based on a luminescence study of water/non-aqueous solvent mixtures of Eu^{3+}, it has previously been determined that N-H vibrations in solvents, like Fm, contribute slightly to deexciting Eu^{3+} when it is excited, but that H_2O was a much more effective quencher[1787]. Eu^{3+} has also been shown to be solvated preferentially by solvents with high enough value of dipole moment instances and donor numbers, as solvation is mainly due to ion-dipole interaction and donor-acceptor interaction[178]. Electrochemically speaking, Fm can also form a weak complex with Eu^{3+}, and in high Fm concentrations (>60%), the reduction of Eu^{3+} to Eu^{2+} was reversible[179].

Further investigation would be required to determine the exact interactive role that Fm has in this hydrogel, and its importance in the ammonia responsiveness of the system, but it is evident that it is the required solvent for ammonia responsiveness.

4.4.7 Freeze Drying

The initial fabrication protocol for the production of the hydrogel requires the use of a freeze-dryer [148]. Since the freeze-thaw method was rendered non-reproducible, a freeze dryer was constructed. A commercial freeze dryer was available for use in the McMaster Biointerfaces Institute, but restrictions on sample solvent were limited to aqueous, thus eliminating the possibility of use of the instrument.

The main components of a freeze dryer are a vacuum pump (Edwards), a sample chamber, and a condensing chamber. The vacuum (Vevor) and insulation pots were purchased from Amazon, the pressure gauge was purchased from Yellow Jacket (Omni Vacuum Gauge) tubing, connectors, washers, insulation, and JB Weld were purchased from Home Depot.

Figure 34. Setup of constructed freeze-dryer. Left to right, Edwards vacuum pump, condensing chamber, sample chamber.

The setup is shown in Figure 34. A hole was drilled in the top of the condenser chamber pot to connect tubing leading to the sample chamber, which was sealed with JB Weld and tested under vacuum. Insulation was layered and glued around the insulator pot, which contained the condensing chamber.

To test the function of the freeze dryer, raspberries were freeze dried. Raspberries were placed in the sample chamber and the lid was placed on. Anhydrous ethyl alcohol 100% (purchased from ABB Lab Stores) was poured into the insulator pot and dry ice (purchased from ABB Lab Stores) was placed in the alcohol. Insulation was placed above the alcohol surrounding the condenser pot inside the insulator pot. The vacuum was turned on and the sample was checked every hour to top up the dry ice and alcohol. A minimum pressure of 234 microns was achieved. After 12h, the vacuum was turned off and left to vent, then raspberries were removed from the sample chamber and observed as successfully freeze-dried (Figure 35).

Figure 35. Successfully freeze-dried raspberries dried with constructed freeze-dryer.

A sample of hydrogel mixture was prepared, poured into a medium petri dish, frozen at -80^{O}C for 12h, then placed in the sample chamber, and the lid was placed on. Anhydrous ethyl alcohol 100% was poured into the insulator pot, dry ice was placed in the alcohol, and insulation was placed to surround the condenser pot. The vacuum was turned on. Bubbles were immediately observed rising from the hydrogel. Alcohol and dry ice were repeatedly topped up as the sample was set to dry for 12h. After 12h, the vacuum was turned off and left to vent, and the sample was removed from the chamber to be observed. The hydrogel was still liquid, indicating that physical crosslinking was not achieved. This is expected to be caused by insufficient consistent low temperatures, potentially coupled with a vacuum pressure which is not sufficient. There is no data available online which gives the required pressure for the triple point of Fm.

4.4.8 PDMS Cap

Despite the gel being unsuccessful, the production of a PDMS cap was explored. Upon consultation with a previous graduate student in the Biophotonics Lab, Colleen Chau, a simple modification to reduce the water contact angle of water with PDMS was determined[129]. For the mold of the PDMS cap, the idea of a 3D printed master was investigated. Surface modification of PLA would be necessary to reduce the grooves created during multiple layers of printer filament. Chemical and physical modifications were both determined as possibilities.

4.5 Conclusion

This work was a step towards the development of a point-of-care, low-cost method for monitoring water, but needs improvement for it to become a practiced method of detection. A protocol needs to be designed to ensure the reproducibility of the ammonia responsive hydrogel being fabricated successfully. It is difficult to say whether this method is feasible until the production of the hydrogel is successfully reproducible, however the fluorescence recovery capabilities of the gel would also need to be further explored and optimized for a higher degree of recovery, so that the quality of subsequent measurement data is not decreased with each measurement. The adhesion of the gel to a microscope slide would also need to be improved, potentially by adding a thin layer of PDMS on the glass before the addition of the hydrogel.

Learned from my work is that Fm is the essential solvent for the production of this hydrogel, as other solvents, while increasing mechanical stability, proved to have no ammonia response. Also learned from my work is the need for a study on the triple point requirements of Fm.

4.6 Future Direction

The feasibility of this detection method, when compared to the previously proposed method, has potential to improve on the low-cost nature of the detection mechanism. To reduce costs even further, a UV filtering plastic could be used in place of a UV filter to reduce excitation light interference. If a reproducible protocol can be established, and the fluorescence recovery mechanism can be improved, this method could be used in multiple applications.

With regards to the detection device for *Cryptosporidium* and *Giardia*, since the Raspberry Pi camera is in contact with the microfluidic channel, the field of view is small compared to the entire device. This makes it challenging for overall fluorescence quenching measurements to be taken. For the (oo)cyst detection device to be successful, it must have a small field of view to detect the small sized (oo)cysts, so increasing the field of view would render the (oo)cyst detection mechanism unusable. A bridge would need to be gapped for the hydrogel to be implemented into the (oo)cyst monitoring system, that allows for the entire intensity measurement to be taken, perhaps by a separate light intensity sensor than the camera used for imaging the (oo)cysts. A potential direction for this would be to image the (oo)cysts with the same UV light as used to excite the ammonia hydrogel. If successful, the same light source could be used to image the (oo)cysts as to excite the hydrogel, and with a filter to block out excitation light, a separate intensity sensor could be employed to detect the fluorescence quenching without the interference of excitation light.

130. Mahoney, e., Xiong, B., Schellhorn, H., Selvaganapathy, R., Fang Q. *Fluorescence-Based Ammonia and Creatinine Sensing for Environmental and Point of Care Monitoring (Chapter 5)*.

131. Xiong B, Mahoney E, Lo JF, Fang Q. A Frequency-Domain Optofluidic Dissolved Oxygen Sensor with Total Internal Reflection Design for in Situ Monitoring. *IEEE Journal of Selected Topics in Quantum Electronics*. 2021;27(4). doi:10.1109/JSTQE.2020.2997810

132. Šraj LO, Almeida MIGS, Swearer SE, Kolev SD, McKelvie ID. Analytical challenges and advantages of using flow-based methodologies for ammonia determination in estuarine and marine waters. *TrAC Trends in Analytical Chemistry*. 2014;59:83-92. doi:10.1016/j.trac.2014.03.012

133. Li D, Xu X, Li Z, Wang T, Wang C. Detection methods of ammonia nitrogen in water: A review. *TrAC - Trends in Analytical Chemistry*. 2020;127:115890. doi:10.1016/j.trac.2020.115890

134. Jones JG, Simon BM, Roscoe J v. Microbiological Sources of Sulphide in Freshwater Lake Sediments. *Microbiology (N Y)*. 1982;128(12):2833-2839. doi:10.1099/00221287-128-12-2833

135. Rusydi AF, Onodera SI, Saito M, et al. Potential sources of ammonium-nitrogen in the coastal groundwater determined from a combined analysis of nitrogen isotope, biological and geological parameters, and land use. *Water (Switzerland)*. 2021;13(1). doi:10.3390/w13010025

136. van Damme M, Clarisse L, Whitburn S, et al. Industrial and agricultural ammonia point sources exposed. *Nature*. 2018;564(7734):99-103. doi:10.1038/s41586-018-0747-1

137. Wakida FT, Lerner DN. Non-agricultural sources of groundwater nitrate: a review and case study. *Water Res*. 2005;39(1):3-16. doi:10.1016/j.watres.2004.07.026

138. Ye J, Chen X, Chen C, Bate B. Emerging sustainable technologies for remediation of soils and groundwater in a municipal solid waste landfill site – A review. *Chemosphere*. 2019;227:681-702. doi:10.1016/j.chemosphere.2019.04.053

139. Liang Y, Yan C, Guo Q, Xu J, Hu H. Spectrophotometric determination of ammonia nitrogen in water by flow injection analysis based on NH3- o-phthalaldehyde -Na2SO3 reaction. *Anal Chem Res*. 2016;10:1-8. doi:10.1016/j.ancr.2016.10.001

140. Cheng Q, Hao A, Xing P. Stimulus-responsive luminescent hydrogels : Design and applications. *Adv Colloid Interface Sci*. 2020;286:102301. doi:10.1016/j.cis.2020.102301

141. Kamoun EA, Chen X, Mohy MS, Kenawy E refaie S. Crosslinked poly (vinyl alcohol) hydrogels for wound dressing applications : A review of remarkably blended polymers. *Arabian Journal of Chemistry*. 2015;8(1):1-14. doi:10.1016/j.arabjc.2014.07.005

142. Ma W peng, Yan B. Lanthanide functionalized MOF thin films as effective luminescent materials and chemical sensors for ammonia†. *Royal Society Of Chemistry*. Published online 2020:15663-15671. doi:10.1039/d0dt03069d

143. Zhang Z, Zhao Z, Lu Y, Wang D, Wang C, Li J. One-Step Synthesis of Eu 3 + - Modified Cellulose Acetate Film and Light Conversion Mechanism. *Polymers (Basel)*. Published online 2021:1-16.

144. Nan P, Orcid ZHU. Self-healing All-in-one Energy Storage for Flexible Self-powering Ammonia Smartsensors. *Energy & Environmental Materials*. 2021;5(3):986-995. doi:10.1002/eem2.12227

145. Kunduru KR, Kutcherlapati SNR, Arunbabu D, Jana T. *Armored Urease : Enzyme-Bioconjugated Poly (Acrylamide) Hydrogel as a Storage and Sensing Platform*. Vol 590. 1st ed. Elsevier Inc.; 2017. doi:10.1016/bs.mie.2017.02.008

146. Yudhana A, Mukhopadhyay S, Ardiansyah OD, Akbar SA, Nuraisyah F, Mufandi I. Multi sensor application-based for measuring the quality of human urine on first-void urine. *Sens Biosensing Res*. Published online 2021:100461. doi:10.1016/j.sbsr.2021.100461

147. Wang Y, Zhang W. Fluorescent color conversion of luminous hydrogel upon stimulation of basic molecule. *J Photochem Photobiol A Chem*. 2019;385(September):112086. doi:10.1016/j.jphotochem.2019.112086

148. Xu Y, Zhang X, Zhang W, Liu X, Liu Q. Fluorescent Detector for NH3 based on Responsive Europium(III)–Salicylic acid Complex Hydrogels. *J Photochem Photobiol A Chem*. 2021;404(September 2020):112901. doi:10.1016/j.jphotochem.2020.112901

149. Wang Y, Zhang W, Li J, Fu J. A novel LEuH/PVA luminescent hydrogel with ammonia response and self-recovery luminescence behavior. *New Journal of Chemistry*. 2019;43(13):5133-5138. doi:10.1039/C9NJ00446G

150. Barkleit A, Acker M, Bernhard G. Europium(III) complexation with salicylic acid at elevated temperatures. *Inorganica Chim Acta*. 2013;394:535-541. doi:10.1016/j.ica.2012.09.014

151. Yang S, Tang Z, Tian Y, et al. Dual-Color Fluorescent Hydrogel Microspheres Combined with Smartphones for Visual Detection of Lactate. *Biosensors (Basel)*. 2022;12(10):1-11. doi:10.3390/bios12100802

152. Xie L, Liu C, Ma L, et al. A unique delaminated MoS4/OS-LEuH composite exhibiting turn-on luminescence sensing for detection of water in formamide. *Dalton Transactions*. 2017;46(10):3110-3114. doi:10.1039/c6dt04870f

153. Simon D, Obst F, Haefner S, et al. Hydrogel/enzyme dots as adaptable tool for noncompartmentalized multi-enzymatic reactions in microfluidic devices. *Royal Society Of Chemistry*. Published online 2019:67-77. doi:10.1039/c8re00180d

154. Abdullah ZW, Dong Y, Davies IJ, Barbhuiya S. PVA , PVA Blends , and Their Nanocomposites for Biodegradable Packaging Application. *Polym Plast Technol Eng*. 2017;0(0):1-38. doi:10.1080/03602559.2016.1275684

155. Solutions LWT. Europium - Eu Chemical properties of europium - Health effects of europium - Environmental effects of europium. Published 1998. https://www.lenntech.com/periodic/elements/eu.htm#:~:text=Europium poses no environmental threath,a fire and explosion hazard.

156. Wang M, Bai J, Shao K, et al. Review Article Poly (vinyl alcohol) Hydrogels : The Old and New Functional Materials. 2021;2021.

157. Bates, N., Puy, C., Jurney, P., McCarty, O., Hinds M. Evaluation of the Effect of Crosslinking Method of Poly (Vinyl Alcohol) Hydrogels on Thrombogenicity. 2020;11(4):448-455. doi:10.1007/s13239-020-00474-y

158. Huang X, Guo Q, Zhou P, Lu C, Yuan G, Chen Z. Poly (vinyl alcohol)/ artificial marble wastes composites with improved melt processability and mechanical properties. *Composites Part B*. 2020;182(October 2019):107628. doi:10.1016/j.compositesb.2019.107628

159. Yan J, Tian H, Zhang Y, Xiang A. Effect of urea and formamide plasticizers on starch / PVA bioblend sheets. 2015;42311(117):1-8. doi:10.1002/app.42311

160. Jiang X, Li C, Han Q. Modulation of swelling of PVA hydrogel by polymer and crosslinking agent concentration. *Polymer Bulletin*. 2022;(0123456789). doi:10.1007/s00289-022-04116-2

161. Onyari JM, Huang SJ. Synthesis and Properties of Novel Polyvinyl Alcohol – Lactic Acid Gels. Published online 2009. doi:10.1002/app

162. Gohil JM, Bhattacharya A, Ray P. Studies on the Cross-linking of Poly (Vinyl Alcohol). Published online 2006:161-169. doi:10.1007/s10965-005-9023-9

163. Patacho I, Oliveira AS, Nolasco P, Colaço R, Ana P. Annals of Medicine Chemically crosslinked PVA hydrogels for cartilage substitution. Published online 2021. doi:10.1080/07853890.2021.1896893

164. Otsuka E, Suzuki A. A Simple Method to Obtain a Swollen PVA Gel Crosslinked by Hydrogen Bonds. Published online 2009. doi:10.1002/app

165. Sanchez LM, Shuttleworth PS, Waiman C, Zanini G, Alvarez VA, Ollier RP. Journal of Environmental Chemical Engineering Physically-crosslinked polyvinyl alcohol composite hydrogels containing clays , carbonaceous materials and magnetic nanoparticles as fi llers. *J Environ Chem Eng*. 2020;8(3):103795. doi:10.1016/j.jece.2020.103795

166. Hassan CM, Peppas NA. Structure and Morphology of Freeze / Thawed PVA Hydrogels. Published online 2000:2472-2479.

167. Lu T, Hixon KR, William J. A combined effect of freeze – thaw cycles and polymer concentration on the structure and mechanical transparent PVA gels. doi:10.1088/1748-6041/7/1/015006

168. Stauffer SR, Peppast NA. Poly (vinyl alcohol) hydrogels prepared by freezing-thawing cyclic processing. 1992;33(18):3932-3936.

169. Nakano T, Nakaoki T. Coagulation size of freezable water in poly (vinyl alcohol) hydrogels formed by different freeze / thaw cycle periods. 2011;(December 2010):875-880. doi:10.1038/pj.2011.92

170. Takigawa T, Kashihara H, Urayama K, Masuda T. Structure and mechanical properties of poly(vinyl alcohol) gels swollen by various solvents. 1992;33(11):2334-2339.

171. Porous Polyvinyl Alcohol Freeze-Thaw Hydrogel. Published online 1999.

172. Melad O, Romiya M. Effect of solvent on the compatibility of polyvinyl alcohol and polymethylmethacrylate by dilute solution viscometry method. *Polymer Science - Series A*. 2015;57(5):622-627. doi:10.1134/S0965545X15050144

173. Gupta K, Patra AK. A luminescent ph-responsive ternary europium(Iii) complex of β-diketonates and terpyridine derivatives as sensitizing antennae – photophysical aspects, anion sensing, and biological interactions. *Eur J Inorg Chem*. 2018;2018(18):1882-1890. doi:10.1002/ejic.201701495

174. Baek NS, Nah MK, Kim YH, Kim HK. Ln(III)-cored complexes based on 2-thenoyltrifluoroacetone ligand for near infrared emission: Energy transfer pathway and transient absorption behavior. *J Lumin*. 2007;127(2):707-712. doi:10.1016/j.jlumin.2007.03.020

175. Gao B, Zhang W, Zhang Z, Lei Q. Preparation of polymer-rare earth complex using salicylic acid-containing polystyrene and its fluorescence emission property. *J Lumin*. 2012;132(8):2005-2011. doi:10.1016/j.jlumin.2012.01.055

176. Shen CQ, Yan TL, Wang YT, Ye ZJ, Xu CJ, Zhou WJ. Synthesis, structure and luminescence properties of binary and ternary complexes of lanthanide (Eu3+, Sm3+ and Tb3+) with salicylic acid and 1,10-phenanthroline. *J Lumin*. 2017;184:48-54. doi:10.1016/j.jlumin.2016.12.018

177. Sharma G, Narula AK. Eu3+-doped CaF2 nanoparticles functionalized by salicylic acid: synthesis, structural, optical and morphological studies. *Journal of Materials Science: Materials in Electronics*. 2016;27(5):4928-4934. doi:10.1007/s10854-016-4377-9

178. Kimura T, Nagaishi R, Kato Y, Yoshida Z. Luminescence study on preferential solvation of Europium(III) in water/non-aqueous solvent mixtures. *J Alloys Compd*. 2001;323-324:164-168. doi:10.1016/S0925-8388(01)01121-5

179. Rabockai T, Jordan I. Electrochemistry of Europium in Aqueous and Aqueous Formamide Solutions. *Anal Lett*. 1974;7(10):647-658. doi:10.1080/00032717408059025

5.1 Conclusion

Water quality monitoring is an important part of our future, especially in a natural resource rich country such as Canada. Safe water for all in Canada should be a basic right, but for so many people, especially Indigenous people and those in remote communities, it is unavailable[1,3,5,119]. The first step towards safe water for all is assessing and evaluating already available water, which can be done through water quality monitoring. Through this thesis, water quality monitoring was explored. From *Cryptosporidium* and *Giardia* detection methods, to ammonia sensitive hydrogels, efforts are being made towards developing low-cost, point-of-care devices capable of providing data on the safety of a water source.

Literature review of *Cryptosporidium* and *Giardia* detection mechanisms proved a starting point for the development of a shadow imaging and flow analysis-based device. Comparison to prior established methods of detection can help identify where their improvements need to be made and allow for better design of further methods. Low-cost, point-of-care detection mechanisms are being developed to reduce the reliance upon expensive lab infrastructure and trained scientists, as well as the cost associated with testing a water sample. With the low-cost, point-of-care detection methods, water quality monitoring can be brought to remote and Indigenous communities, as well as any community which does not have access to testing infrastructure.

Ground truth images of *Cryptosporidium* and *Giardia* (oo)cysts were taken to establish a set of images to reference when building the algorithm for tracking the movement of the (oo)cysts within a microfluidic channel. Non-human infective models of (oo)cysts (*Giardia lamblia* and *Cryptosporidium parvum*, gamma irradiated) were chosen to undergo baseline microscopic imaging, advantageous for their lack of infectivity. For further studies *Cryptosporidium hominis*, the most human infective species, could be chosen to provide more accurate morphological features towards detecting the most human infective model. With the morphology data gathered from these images, an algorithm to track the particles through the channel can be built by analyzing the flow mechanics of an identically shaped particle.

The first steps towards fabricating an ammonia responsive hydrogel to implement with the detection of *Cryptosporidium* and *Giardia* were taken. Based on these experiments, further steps would need to be made to ensure the hydrogel has a reproducible protocol, as well as further investigation into the fluorescence recovery mechanism would need to be done to improve the rate of recovery. Learned from my work is that Formamide is the essential solvent for maintaining ammonia responsiveness in the hydrogel. The proposed solution has the potential to be a low-cost fabrication and detection method for aqueous ammonia monitoring, which can be combined with other microfluidic devices to detect ammonia in tandem with other targets of interest.

The water quality monitoring applications of the device proposed in this thesis would reduce transportation costs, labour, and the need for expensive lab infrastructure to monitor water in remote locations. The device also has the capability to be adjusted to monitor urine for healthcare purposes, such as ammonia in urine or for the presence of urine sediment. Both healthcare applications and water quality monitoring applications are beneficial not only to the general Canadian population, but especially to those where the access to healthcare and water quality infrastructure is limited. The information presented in this thesis is a contribution to the goal of bringing low-cost water monitoring and healthcare devices to all.

1. McKitrick Ross, Aliakbari Elmira, Stedman Ashley. *Evaluating the State of Fresh Water in Canada*. (Aliakbari Elmira, McKitrick Ross, Stedman Ashley, eds.). Fraser Institute; 2018.

3. Bakker K, Cook C. Water Governance in Canada: Innovation and Fragmentation. *Water Resources Development*. 2011;27:275-289. doi:10.1080/07900627.2011.564969

5. Wilson NJ, Montoya T, Arseneault R, Curley A. Governing water insecurity: navigating indigenous water rights and regulatory politics in settler colonial states. Published online 2021. doi:10.1080/02508060.2021.1928972

119. Mcgregor D. *The Ethic of Responsibility*.; 2014.